Research Plan for Spin Physics at RHIC

Abstract

1 Executive Summary (by *Gerry*)

Briefly describe the physics case/highlights of the RHIC Spin program, the detector and accelerator capabilities and their development, and the plans over the next few years.

In this report we present our research plan for the RHIC spin program. The Department of Energy's Office of Nuclear Physics Science and Technology Review Committee, in their report of September 2004, recommended preparation of a plan that covers 1) the science of RHIC spin, also in the context of work world-wide; 2) the requirements for the accelerator; 3) resources that are required including timelines; and 4) the impact of a constant effort budget to the program. The RHIC Spin Plan Group was charged by Thomas Kirk, BNL Associate Director for High Energy and Nuclear Physics, to create this plan.

The RHIC spin physics program contributes to a developing understanding of the known matter in our universe. This matter is predominantly nucleons, protons and neutrons of atomic nuclei. Deep inelastic scattering of high energy electrons from protons established in the 1960s that the nucleons are built from quarks.Quantum chromodynamics (QCD) is now believed to be the theory of the nuclear force, with protons built from quarks and the QCD force carrier, the gluons.Unpolarized studies have verified many predictions of QCD, probing deeply inside the proton using unpolarized colliders at very high energy. These experiments have determined with great precision the unpolarized structure of the nucleons, the distributions of quarks, gluons, and anti-quarks.

There has also been considerable progress, and a major surprise, studying the spin structure of the nucleons. *Polarized* deep inelastic experiments (DIS) from the 1980s to now, done at the SLAC, CERN, and DESY accelerator laboratories, have shown that the quarks and anti-quarks in the proton and neutron carry very little of the spin of the nucleon, on average. Roughly 75% of the nucleon spin must be carried by its gluons and by orbital angular momentum. This was seen as quite surprising in 1989 when it was first discovered. Although the QCD theory does not yet provide predictions for this structure, it was expected that the quarks would carry the nucleon spin. This polarized DIS result indicated that the proton and neutron have surprising spin structure, and probing this structure has become a major focus in our field.

The DIS experiments probe the nucleon using the electromagnetic interaction. The electromagnetic interaction scatters through electric charge, directly observing the effect of the charged quarks and anti-quarks in the nucleon, but not the electrically-neutral gluons.

The RHIC spin program, colliding polarized protons at $\sqrt{s}$=200 GeV and above, uses the strongly interacting quarks and gluons from one colliding proton to probe the spin structure of the other proton. The RHIC program is particularly sensitive to the gluon polarization in the proton, which will be independently measured with several processes. In addition, parity-violating production of W bosons at RHIC will offer an elegant method to directly measure the quark and anti-quark contributions to the proton spin, sorted by type of quark. These measurements explore the structure of longitudinally polarized protons. The transverse spin structure of the proton can be different from longitudinal, and this is also a major topic at RHIC, and large spin asymmetries have already been observed.

The RHIC spin program is underway. Highly polarized protons, P=45%, have been success-

fully accelerated to 100 GeV, using unique sets of magnets called Siberian Snakes in the RHIC accelerator. The first polarized collisions at $\sqrt{s}$=200 GeV took place in 2001, and polarization and luminosity have been increased substantially since then. The RHIC spin accelerator complex includes a new polarized source providing very high intensity polarized (P=80%) H^- ions, new "partial" Siberian Snake magnets in the AGS accelerator, four "full" Siberian Snakes in RHIC, and eight sets of Spin Rotator magnets in RHIC. Polarization is measured with new devices in the LINAC accelerator, the AGS, and in RHIC. Absolute polarization was determined at 100 GeV using a polarized atomic hydrogen gas "jet" target in RHIC in 2004. Progress in polarization and luminosity has been made by combining machine work with periods of sustained collisions for physics.

The two large RHIC detectors, PHENIX and STAR, have photon, electron, charged hadron, and muon detectors, all important for the spin program. Measurements of the unpolarized cross sections for π^0 and direct γ production, reported by the RHIC experiments, are described well by QCD predictions. These predictions are based on a perturbative expansion of QCD and calculations have been carried out to two orders for all important RHIC spin processes. Theoretical understanding of these important probes for spin physics at RHIC is robust. First spin measurements from RHIC have been published, showing a large spin asymmetry for π^0 produced in the collision of transversely polarized beams, and a helicity asymmetry for π^0 production, sensitive to gluon polarization, consistent with zero.

We now summarize our findings on the four areas in the charge.

Science. Gluon polarization will be measured at RHIC using several independent methods: π^0, jet, direct γ and γ+ jet, and heavy quark production. Results from the different methods will both overlap to allow us to test our understanding of the processes involved, and expand the range of momentum fraction for the measurements. We want to learn both the average contribution to the proton spin of the gluons, as well as a detailed map. We use first the higher cross section processes, π^0 and jet production, and, as we reach higher luminosity and polarization, the clean but rarer process of direct γ production. We plan to emphasize these measurements for $\sqrt{s}$=200 GeV collisions from 2005-2008. At that time, we expect to have reached a precision that can clearly distinguish between zero gluon polarization and a minimal ("standard") gluon polarization. A large gluon polarization, consistent with the gluon carrying most of the spin of the proton, would be precisely measured. In this period we will also pursue the question of the transverse spin structure. Gluons, massless spin 1 particles, cannot contribute to the transverse spin. Large transverse spin asymmetries have been seen for DIS and now for RHIC, so this topic is also a potential window into a new understanding of the structure of the nucleons.

Production of W bosons, the carrier of the weak interaction, has an inherent handedness. At RHIC we plan to use this "parity violation" signal to directly measure the polarization of the quark and anti-quark that form the W boson. To do this we will run at the top RHIC energy, $\sqrt{s}$=500 GeV. This will provide the first direct measurements of anti-quark polarization in the proton, with excellent sensitivity. We plan to begin these measurements in 2009. The W measurements will require completed detector improvements for both PHENIX and STAR.

The RHIC spin results will provide precise measurements of gluon and anti-quark polarization. With these results we will also understand the role of the remaining contributor to the proton spin, orbital angular momentum. We will have also explored our understanding of the

interconnected results from the different RHIC spin probes, and from the DIS measurements. The sensitivity at RHIC for gluon polarization is shown in Figure 1, where we also include the sensitivity for the ongoing DIS experiment at CERN, which measures gluon polarization by the production of hadrons. From the figure, we see that RHIC will provide precise results over a large range in momentum fraction, characterizing the gluon contribution to the proton spin.

Figure 1: Delta G/G(x) vs. log x with a model, showing the x range for various RHIC processes and with expected uncertainties. Also indicate 200 and 500 GeV data. Include COMPASS expected uncertainties for $Q^2 > 1$.

The sensitivity of RHIC for anti-quark polarization is shown in Figure 2. We will measure the ubar and dbar anti-quark polarization to about ± 0.01, as well as u and d quark polarization. The measurement is direct and very clean, using parity violating production of W bosons. DIS measurements also study anti-quark polarization. The method has the disadvantage of theoretical uncertainties on modeling the fragmentation and the advantage that the method is accessible today. The RHIC and DIS methods probe the proton at very different distances, or Q^2, where RHIC corresponds to X Fermi and DIS to Y Fermi, compared to the proton radius 1 Fermi. The theory of QCD prescribes how to connect the results from different probing distances–the description of unpolarized DIS results over a very large distance range is one of the major successes of QCD. Both the anti-quark and the gluon results from RHIC and DIS test the QCD assumption of universality: the physics for both proton and lepton processes can be described with the same underlying quark, anti-quark, and gluon distributions.

Figure 2: Delta Q/Q(x) vs. log x with a model, for u, d, ubar and dbar. Show RHIC expected uncertainties, DIS (or show A_1^p with DIS measurements and RHIC sensitivities?).

We emphasize that the planned RHIC program will make major contributions to our understanding of matter. Our results will complement the DIS measurements, completed and planned. We include in our report expectations from a next stage of DIS–colliding polarized electrons with polarized protons and neutrons which probes still further into the structure of matter. As we develop theoretical tools to apply QCD to understand this structure, these spin results will provide a deep test of our understanding of the fundamental building blocks of matter.

Performance Requirements. The program requires RHIC beams with high polarization, and high integrated luminosity. For our sensitivities above we have used P=0.7 and luminosity 300 pb^{-1} at $\sqrt{s}$=200 GeV and 800 pb^{-1} at $\sqrt{s}$=500 GeV. (Note that this would be "delivered" luminosity, while the figures would use recorded luminosity. We would make this point in the body of the report.)

The polarization level is presently P=0.45, and is expected to reach 70% polarization by 2006. This improvement is anticipated from new Siberian Snakes installed in the AGS in 2004 and 2005.

The average luminosity at store must be increased by a factor 15 to reach the integrated luminosity goals in three years of running, 10 physics weeks per year. To achieve this will require completion of the planned vacuum improvements in RHIC, expected for 2007. The luminosity increase then comes from reaching a bunch intensity of 2×10^{11}. A limit will be caused by beam-beam interactions that change and broaden the betatron tune of the machine, moving part of the beam into a beam resonance region where beam is then lost. Work in 2004 discovered a new

betatron tune for RHIC that greatly improves loss from the beam-beam interaction. RHIC at our luminosity goal will be above previously reached tune spread limits, and will be close to vacuum limits from the development of electron clouds.

Reaching these goals requires learning by doing. We plan to study limits and develop approaches to improve the polarization and luminosity during physics runs by including beam studies for one shift per day. It is also important that a sustained period of running and development be followed, if possible each year. It is this approach that has led to the major improvements for heavy ion luminosity and to our improvements to this date in polarization and proton luminosity.

Experiment Resources. The PHENIX and STAR detectors are complete, for the gluon polarization program. Improvements to both detectors are required to carry out the W physics program. Both experiments also plan upgrades that benefit both the heavy ion and spin programs, significantly extending the range of physics probes for spin.

PHENIX. The present online event selection for muons, the channel used for W physics, will need to be improved for the W luminosity. New resistive plate chambers (RPC) are being proposed to provide the tighter event selection, along with electronics changes to the muon tracking readout. The RPC proposal was submitted to NSF in January 2005, with a cost estimate of $1.8M. The tracking readout proposal has been submitted to the Japan Society for the Physical Sciences, with a cost of $1.0M. The planned timeline for both is to complete for the 2008 run.

STAR. New tracking for forward electrons from W decay is necessary for the W program. It is planned to propose this upgrade in 2006 to DOE, with an estimated cost of $5M, although research and development on the technology (GEM detectors) is proceeding and the cost estimate is rough at this time. The forward tracking detector is to be completed for the 2010 run, with part of the detector in place earlier.

Heavy Ion/Spin Upgrades–PHENIX. PHENIX plans a barrel micro vertex detector which gives access to heavy quark states and to jet physics based on tracking. The heavy quark data will add a new probe for gluon polarization at lower momentum fraction (shown on Fig. 1). The jet information will be used in correlated (γ+jet) measurements, which better determine the subprocess kinematics for gluon polarization measurement. A second upgrade being planned is to change the brass "nose cones", used as a filter for the muon arms, to active calorimeters that will measure photons, π^0 and jet energy. The nose cone calorimeters would provide a larger momentum fraction range for the gluon polarization measurements. Both are important upgrades for the heavy ion physics program. The vertex detector is planned for the 2008 run, and the nose cone calorimeter proposal is being developed now.

Heavy Ion/Spin Upgrades–STAR. Expanded forward calorimeters are being proposed for STAR to NSF in January 2005. The calorimeters will measure the gluon density for proton-gold collisions, and will also provide very significant spin measurements. With the calorimeters, forward π^0, γ, and jet events can be observed, giving sensitivity to gluon polarization at lower momentum fraction, as shown on Fig. 1. A second upgrade driven by the heavy ion program, a barrel inner tracker, will give access to heavy quark measurements for spin. The forward calorimeters are to be in place for the 2007 run. The barrel inner tracker is to be completed for the 20?? run.

To summarize, the muon trigger improvements for PHENIX and the forward tracking upgrade for STAR are necessary for the W physics program shown in Fig. 2. PHENIX expects to be ready

for a full 500 GeV program by 2009, and STAR expects to have part of its detector ready for 2009, and the full tracker for 2010. Heavy ion/spin upgrades are being planned that significantly expand the range and sensitivity for spin measurements.

Impact of 10 and 5 Physics Weeks per Year We have been requested in the charge to consider two scenarios: 10 and 5 spin physics weeks per year. We would like to emphasize that we expect the actual running plan to be developed from the experiment beam use proposals. Our consideration of these scenarios should not suggest that we advocate a change to this successful approach.

We show in Fig. 3 the impact of 10 and 5 spin physics weeks per year. The "target" represents the luminosity used for the sensitivities shown in the figures above. With 10 weeks per year, we achieve the $\sqrt{s}$=200 GeV target in 3 years, where we assume that we successfully climb the learning curve to reach the target store luminosity. The 500 GeV running target is also expected to be achieved in 3 years (there is a natural luminosity improvement for 500 GeV of a factor of 2.5 over 200 GeV from the smaller cross section beams).

With 10 spin physics weeks per year, our proposed target sensitivities can be reached running at $\sqrt{s}$=200 GeV from 2005-2008, and at $\sqrt{s}$=500 GeV from 2009-2012, where we have assumed that 2009 will be an "engineering" year, learning to handle the high luminosity and to commission the new detectors. This is our proposal.

As can be seen in Fig. 3, running 5 spin physics weeks per year (we have interpreted this as running 10 spin physics weeks every two years to improve end effects), each program, 200 GeV and 500 GeV, takes more than 6 years. Under this scenario RHIC would run roughly 25% of the year, and both the heavy ion and spin programs would be stretched a factor of greater than two in calendar time.

Fig. 3: pp luminosity projections for 10 and 5 physics weeks per year (5=10/2).

2 The case for RHIC Spin

2.1 Introduction: what we have learned so far (Werner – still very much under construction! I have more, but it's not in yet.)

Spin physics at RHIC has largely been motivated by the exciting and unexpected results from the tremendously successful experimental program on polarized deeply-inelastic scattering over the last $\sim$ 30 years. At the center of attention was the nucleon's spin structure function $g_1(x, Q^2)$. These data have provided much interesting information about the nucleon and QCD. They have given direct access to the helicity-dependent parton distribution functions of the nucleon,

$$\Delta f(x, Q^2) = f^+ - f^- \qquad (f = q, \bar{q}, g) \ , \tag{1}$$

which count the numbers of partons with same helicity as the nucleon, minus opposite. Fig. 1 shows a recent compilation [**?**] of the world data on $g_1(x, Q^2)$, and results of a recent analysis of those data in terms of the Δf.

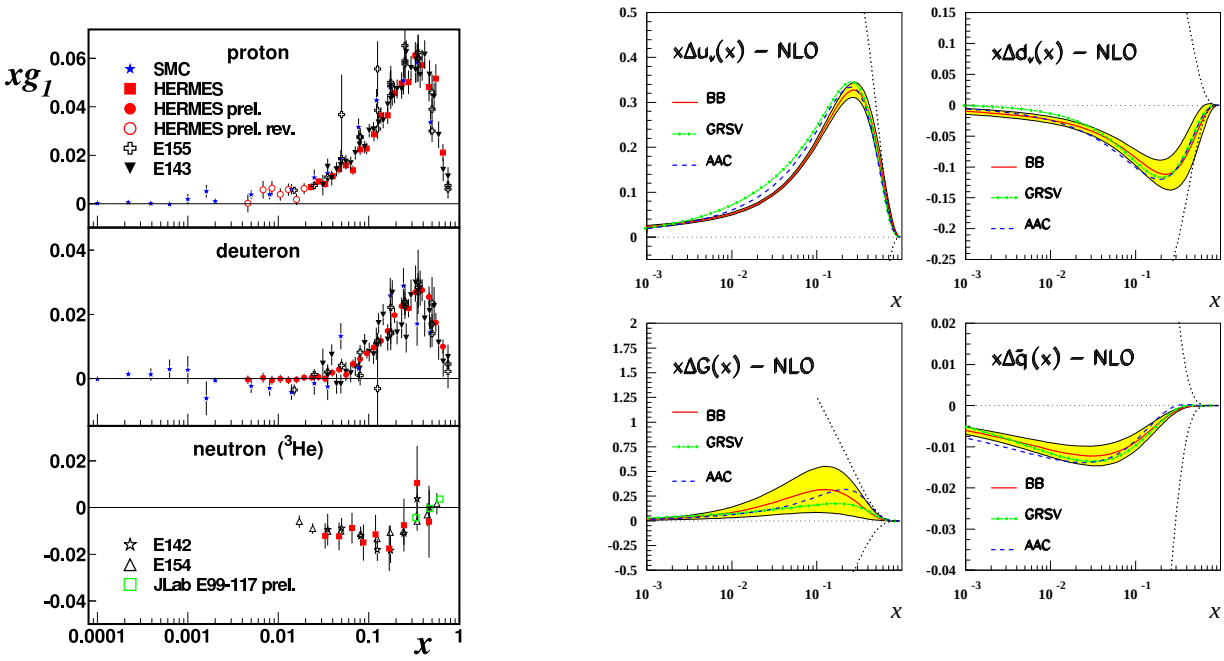

Figure 1: Left: data on the spin structure function g_1, as compiled and shown in [**?**]. Right: analysis of polarized DIS in terms of spin-dependent parton densities of the nucleon. The shaded bands display the current uncertainties (statistical only) [**?**].

Polarized DIS actually measures the combinations $\Delta q + \Delta\bar{q}$. From $x \to 0$ extrapolation of the structure functions for proton and neutron targets it has been possible to test and confirm the Bjorken sum rule [**?**]. Polarized DIS data, when combined with input from hadronic β decays, have allowed to extract the – unexpectedly small – nucleon's axial charge $\sim \langle P|\bar{\psi}\,\gamma^\mu\,\gamma^5\,\psi|P\rangle$, which is identified with the quark spin contribution to the nucleon spin [**?**].

2.2 Compelling questions in spin physics

The results from polarized inclusive DIS have led us to identify the next important goals in our quest for understanding the spin structure of the nucleon. The measurement of gluon polarization $\Delta g = g^+ - g^-$ is a main emphasis at several experiments in spin physics today, since Δg could be a major contributor to the nucleon spin. Also, more detailed understanding of polarized quark distributions is clearly needed; for example, we would like to know about flavor symmetry breakings in the polarized nucleon sea, details about strange quark polarization, the relations to the F, D values extracted from baryon β decays, and also about the small-x and large-x behavior of the densities. Again, these questions are being addressed by current experiments. Finally, we would like to find out how much orbital angular momentum quarks and gluons contribute to the nucleon spin. Ji showed [**?**] that their total angular momenta may be extracted from deeply-virtual Compton scattering, which has sparked much experimental activity also in this area.

- initial information on spin structure of the nucleon, spin "crisis" & spin sum rule
- motivation for studies of gluon polarization Δg and for further studies of quark polarization
- parton angular momenta

• transverse-spin asymmetries, transversity, parton correlations, parton transverse momentum & spin, and what they tell us about the nucleon
• physics of elastic scattering
• wider context of nucleon spin structure
• why polarized pp scattering to answer these questions ? What can it probe ? Complementarity to DIS
(leads into next section)

2.3 Unpolarized pp scattering (Stefan & Werner)

2.3.1 Introduction

The basic concept that underlies most of RHIC spin physics is the factorization theorem [1]. It states that large momentum-transfer reactions may be factorized into long and short-distance contributions. The long-distance pieces contain information on the structure of the nucleon in terms of its distributions of constituents, "partons". The short-distance parts describe the hard interactions of these partons and can be calculated from first principles in QCD perturbation theory. While the parton distributions describe universal properties of the nucleon, that is, are the same in each reaction, the short-distance parts carry the process-dependence and have to be calculated for each reaction considered.

As an explicit example, we consider the cross section for the reaction $pp \to \pi(p_\perp)X$, where the pion is at high transverse momentum $p_\perp$, ensuring large momentum transfer. The statement of the factorization theorem is then:

$$d\,\sigma \;=\; \sum_{a,b,c} \int dx_a \int dx_b \int dz_c \;\; f_a(x_a,\mu) \;\; f_b(x_b,\mu)\, D_c^\pi(z_c,\mu)$$
$$\times\, d\,\hat{\sigma}_{ab}^c(x_a P_A, x_b P_B, P_\pi/z_c, \mu) \;\;, \qquad (2)$$

where the sum is over all contributing partonic channels $a+b \to c+X$, with $d\,\hat{\sigma}_{ab}^c$ the associated partonic cross section. Any factorization of a physical quantity into contributions associated with different length scales will rely on a "factorization" scale that defines the boundary between what is refered to as "short-distance" and "long-distance". In the present case this scale is represented by μ in Eq. (2). μ is essentially arbitrary, so the dependence of the calculated cross section on μ represents an uncertainty in the theoretical predictions. However, the actual dependence on the value of μ decreases order by order in perturbation theory. This is a reason why knowledge of higher orders in the perturbative expansion of the partonic cross sections is important. We also note that Eq. (2) is of course not an exact statement. The factorized structure does become arbitrarily accuracte at very high momentum transfer. At lower momentum transfer, there are corrections to Eq. (2) as such, which are down by innverse powers of the hard scale. These are the so-called "power-suppressed" (or, less precisely, "higher-twist") contributions. They involve interesting physics per se, as we will see for one example in the section on transverse spin below. Concerning the study of parton distribution functions they are to be regarded as "contaminations", and one has to be sure that they are rather unimportant for the kinematics of interest.

Eq. (2) offers the possibility to study nucleon structure, represented by the parton densities $f_{a,b}(x,\mu)$, through a measurement of $d\,\sigma$, hand in hand with a theoretical calculation of $d\,\hat{\sigma}$. In

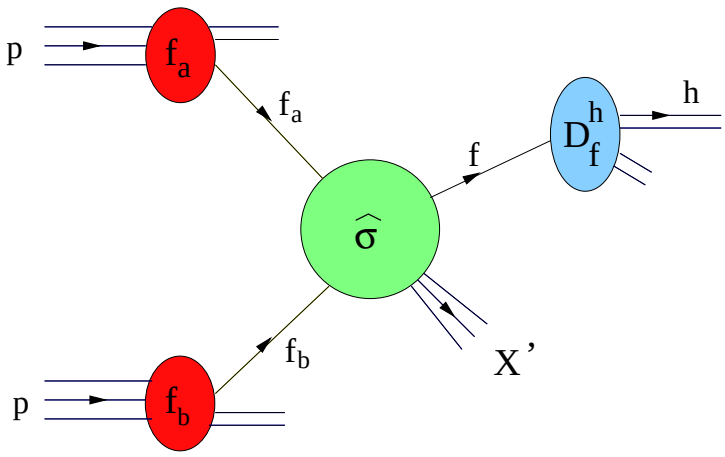

Figure 2: Factorization in terms of parton densities, partonic hard-scattering cross sections, and fragmentation functions.

this particular example, the fact that we are observing a specific hadron in the reaction requires the introduction of additional long-distance functions, the parton-to-pion fragmentation functions D_c^π. These functions have been determined with some accuracy by observing leading pions in e^+e^- collisions and in DIS [2]. A graph such as in Fig. 2 serves as an illustration of QCD factorization [1].

As mentioned above, the partonic cross sections may be evaluated in perturbation theory. Schematically, they can be expanded as

$$d\,\hat{\sigma}_{ab}^{c} \;=\; d\,\hat{\sigma}_{ab}^{c,(0)} + \frac{\alpha_s}{\pi} d\,\hat{\sigma}_{ab}^{c,(1)} + \ldots \;. \tag{3}$$

$d\,\hat{\sigma}_{ab}^{c,(0)}$ is the leading-order (LO) approximation to the partonic cross section. The lowest order can generally only serve to give a rough description of the reaction under study. It merely captures the main features, but does not usually provide a quantitative understanding. The first-order ("next-to-leading order" [NLO]) corrections are generally indispensable in order to arrive at a firmer theoretical prediction for hadronic cross sections. Only with knowledge of the NLO corrections can one reliably extract information on the parton distribution functions from the reaction. This is true, in particular, for spin-dependent cross sections, where both the polarized

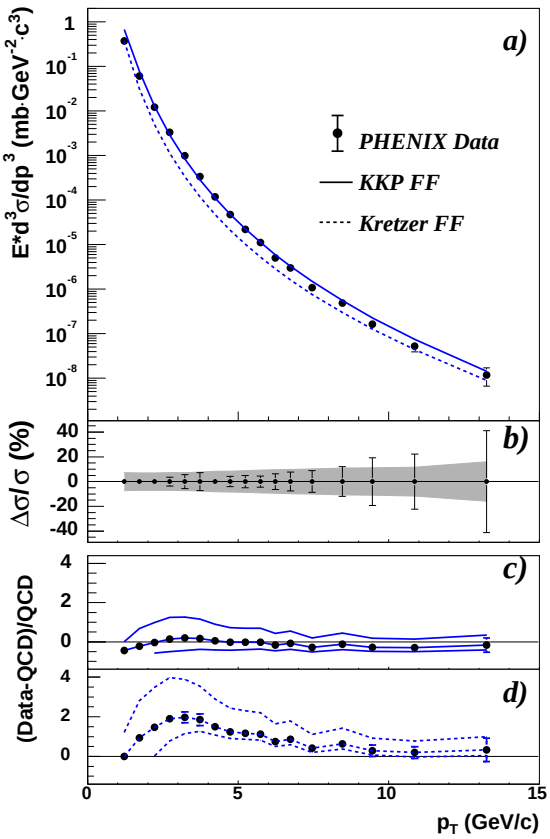

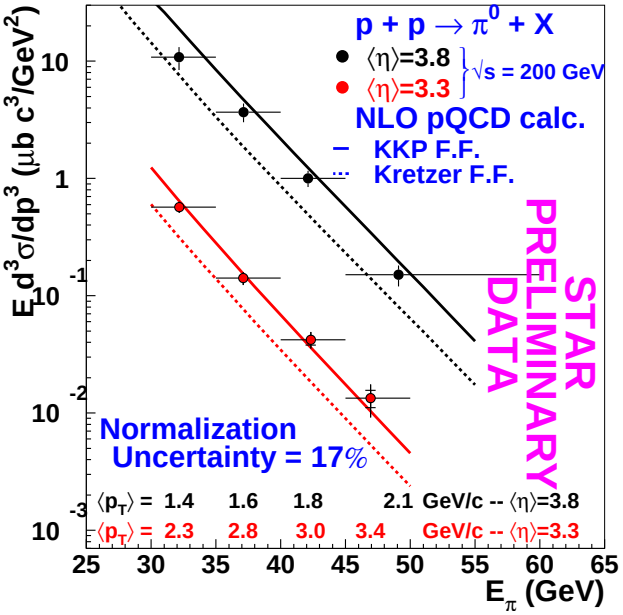

Figure 3: Data from Phenix and STAR for inclusive π^0 production at RHIC.

Figure 4: Data from Phenix for inclusive $pp \to \gamma X$ production at RHIC.

parton densities and the polarized partonic cross sections may have zeros in the kinematical regions of interest, near which the predictions at lowest order and the next order will show marked differences.

There have already been results from RHIC that demonstrate that the NLO framework outlined above is successful. Figure 4 shows comparisons of data from Phenix and STAR for inclusive-pion production $pp \to \pi^0 X$ with NLO calculations. As can be seen, the agreement is excellent at central and forward rapidities, and down even to $p_\perp$ values as low as $p_\perp \gtrsim 1$ GeV. Similar comparisons are shown for prompt-photon production $pp \to \gamma X$ in Fig. **??**, showing a similar level of agreement. We note that such an agreement was not found in previous comparisons of NLO calculations and data in the fixed-target regime. The good agreement of the pion and photon spectra with NLO QCD at RHIC's $\sqrt{S}$, and the good precision of the RHIC data provide a solid basis to extend this type of analysis to polarized reactions. They give confidence that the theoretical hard scattering framework also used for calculations for RHIC spin is indeed adequate.

Fig. 5 decomposes the π^0 cross section at central rapidities into the contributions from the two-parton initial states. It is evident that for $p_\perp \leq 15$ GeV processes with initial gluons dominate by far. This is even more pronounced in case of prompt-photon production, where the Compton process $qg \to \gamma q$ is responsible for more than 90% of the cross section. This implies that such reactions are excellent probes of gluons in the nucleon, and suggests to use them in polarized collisions to learn about gluon polarization. We will now turn to polarized pp collisions at RHIC.

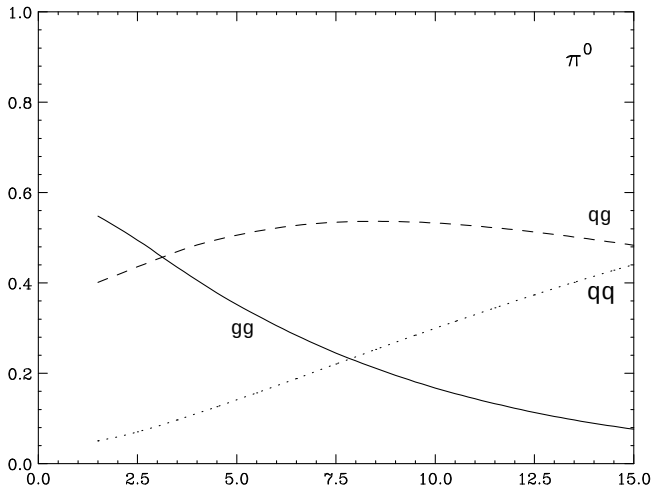

Figure 5: Partonic decomposition of the initial and final state of pp collisions at 200 GeV.

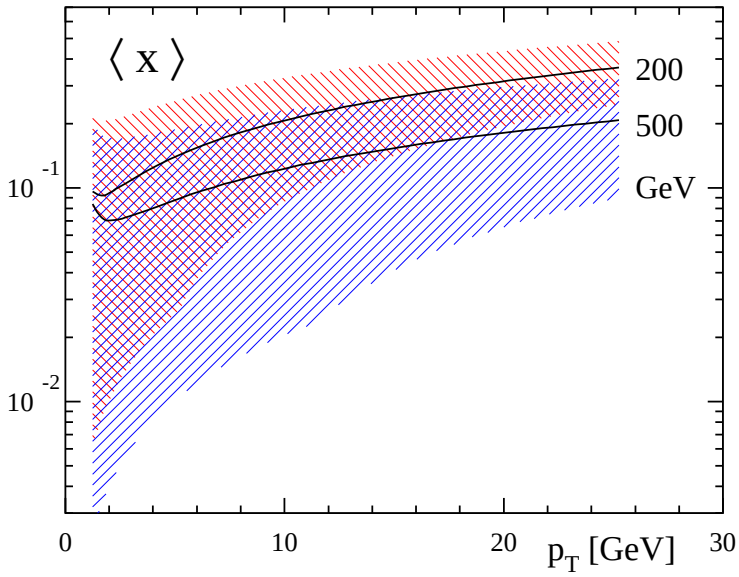

Figure 6: Average values of partonic momentum fractions x at $\sqrt{S} = 200$ and 500 GeV.

2.4 Probing the spin structure of the nucleon in polarized pp collisions (Marco & Werner)

The basic concepts laid out so far for unpolarized inelastic pp scattering carry over to the case of polarized collisions: spin-dependent inelastic pp cross sections factorize into "products" of polarized parton distribution functions of the proton and hard-scattering cross sections describing

spin-dependent interactions of partons. As in the unpolarized case, the latter are calculable in QCD perturbation theory since they are characterized by large momentum transfer. Schematically, one has for the numerator of the spin asymmetry:

$$d\Delta\sigma = \sum_{a,b=q,\bar{q},g} \Delta a \otimes \Delta b \otimes d\Delta\hat{\sigma}_{ab} \,, \tag{4}$$

where $\otimes$ denotes a convolution and where the sum is over all contributing partonic channels $a + b \to c + X$ producing the desired high-p_T or large-invariant mass final state. $d\Delta\hat{\sigma}_{ab}$ is the associated spin-dependent partonic cross section. Eq. (4) equally applies to longitudinal and transverse polarization. In the former case, the parton densities are the helicity distributions introduced in the previous section, and the spin-dependent partonic cross sections are defined as

$$d\Delta\hat{\sigma}_{ab} = d\hat{\sigma}_{ab}(++) - d\hat{\sigma}_{ab}(+-) \,, \tag{5}$$

the signs denoting the helicities of the initial partons a, b. In case of transverse polarization, the parton densities are the transversity distributions to be discussed in more detail below, and the partonic cross sections are defined similar to 5, but for transverse initial polarization. One then customarily uses a small δ to designate polarized quantities instead of a captial one. In this section, we will focus on the longitudinal case; we will return to transverse polarization in the next section.

Since the partonic cross sections are calculable from first principles in QCD, Eq. (4) may be used to determine the polarized parton distribution functions from measurements of the spin-dependent pp cross section on the left-hand side. Another crucial point here is that, as discussed in the previous section, the parton distributions are universal, that is, they are the same in all inelastic processes, not only in pp scattering, but also for example in deeply-inelastic lepton nucleon scattering which up to now has mostly been used to learn about nucleon spin structure. This means that inelastic processes with polarization have the very attractive feature that they probe fundamental and universal spin structure of the nucleon. In effect, we are using the asymptotically free regime of QCD to probe the deep structure of the nucleon, which is clearly nonperturbative.

At RHIC, there are a number of interesting and measurable processes at our disposal. The key ones, some of which will be discussed in detail in the following, are listed in Table 1, where we also give the dominant underlying partonic reactions and the part of nucleon structure they probe. Basically, for each one of these the parton densities enter with different weights, so that each has its own role in helping to determine the polarized parton distributions. Some will allow a clean determination of gluon polarizations, others are more sensitive to quarks and antiquarks. Eventually, when data from RHIC will become available for most or all processes, a "global" analysis of the data, along with information from lepton scattering, will be performed which then determines the $\Delta q, \Delta\bar{q}, \Delta g$.

As we have already mentioned a number of times, the partonic cross sections are calculable in QCD perturbation theory. The sensitivity with which one can probe the polarized parton densities will foremost depend on the weights with which they enter the cross section. Good measures for this are the so-called partonic analyzing powers. The latter are just the spin asymmetries

$$\hat{a}_{LL} = \frac{d\hat{\sigma}_{ab}(++) - d\hat{\sigma}_{ab}(+-)}{d\hat{\sigma}_{ab}(++) + d\hat{\sigma}_{ab}(+-)} \tag{6}$$

Reaction	Dom. partonic process	Pol. parton distrib.	Status & Ref.
$\vec{p}\vec{p} \to \pi + X$	$\vec{g}\vec{g} \to gg$ $\vec{q}\vec{g} \to qg$	Δg	NLO [**?**, **?**]
$\vec{p}\vec{p} \to \mathrm{jet(s)} + X$	$\vec{g}\vec{g} \to gg$ $\vec{q}\vec{g} \to qg$	Δg	NLO [**?**]
$\vec{p}\vec{p} \to \gamma + X$	$\vec{q}\vec{g} \to \gamma q$	Δg	NLO [**?**, **?**, **?**]
$\vec{p}\vec{p} \to \gamma + \mathrm{jet} + X$	$\vec{q}\vec{g} \to \gamma q$	Δg	NLO [**?**, **?**]
$\vec{p}\vec{p} \to \gamma\gamma + X$	$\vec{q}\vec{\bar{q}} \to \gamma\gamma$	$\Delta q, \Delta\bar{q}$	NLO [**?**]
$\vec{p}\vec{p} \to DX, BX$	$\vec{g}\vec{g} \to c\bar{c}, b\bar{b}$	Δg	NLO [**?**]
$\vec{p}\vec{p} \to \mu^+\mu^- X$ (Drell-Yan)	$\vec{q}\,\vec{\bar{q}} \to \gamma^* \to \mu^+\mu^-$	$\Delta q, \Delta\bar{q}$ NNLO	NLO [**?**, **?**, **?**] [**?**]
$\vec{p}\vec{p} \to (Z^0, W^\pm)X$ $p\vec{p} \to (Z^0, W^\pm)X$	$\vec{q}\,\vec{\bar{q}} \to (Z^0, W^\pm)$	$\Delta q, \Delta\bar{q}$	NLO [**?**, **?**, **?**]

Table 1: Key processes at RHIC for the determination of the parton distributions of the longitudinally polarized proton, along with the dominant contributing subprocesses, the parton distribution predominantly probed, and the status of the theoretical calculations for the partonic hard-scattering cross section.

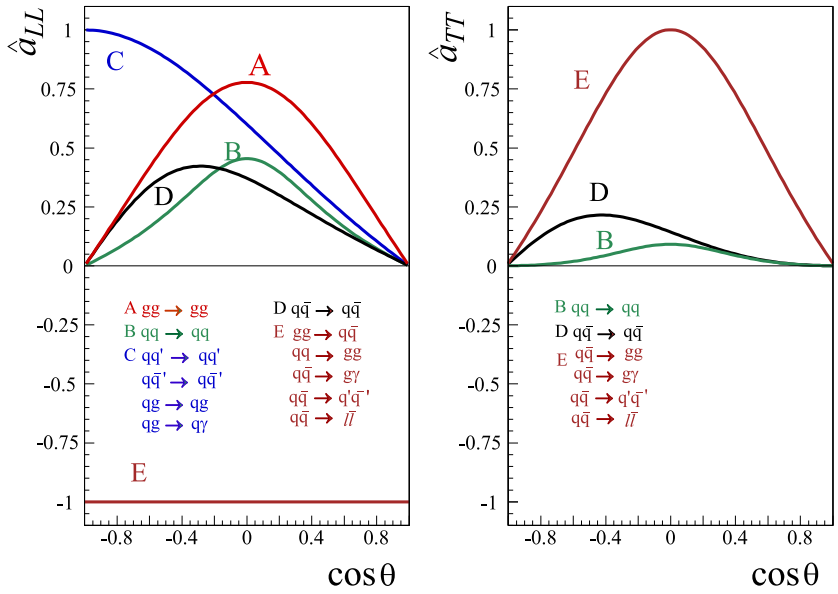

Figure 7: Spin asymmetries for the most important partonic reactions at RHIC at lowest order in QCD. Left: helicity dependence, right: transverse polarization.

for the individual partonic subprocesses. Figure 7 shows these analyzing powers at lowest order for most of the processes listed in Table 1. One can see that the analyzing powers are usually very substantial. For future reference, we also give the subprocess asymmetries for transverse polarization.

It is also very important that the partonic analyzing powers be known accurately. This means that one should include, where available, at least the first-order ("next-to-leading order" (NLO)) QCD corrections to the partonic hard-scattering cross sections. NLO corrections significantly improve the theoretical framework; it is known from experience with the unpolarized case that

the corrections are indispensable in order to arrive at quantitative predictions for hadronic cross sections. Indeed, as we have seen in the preceding subsection, the perturbative framework at NLO leads to an excellent agreement of theory calculations with RHIC high-p_T cross section data in the unpolarized case. The past few years have seen a tremendous progress on the corresponding calculations of NLO corrections for the spin-dependent proceses, with the corrections now known for literally all relevant processes. In some cases, next-to-next-to-leading order (NLLO) corrections are known, and all-order QCD resummations of large perturbative corrections have been applied occasionally. In summary, all tools are in place now for an adequate theoretical treatment the spin reactions relevant at RHIC.

We will now address some of the most important processes in more detail, summarizing theoretical predictions and experimental plans and prospects at RHIC. We will start with those that are sensitive to gluon polarization in the proton, and then discuss W production which will give information about the quark polarizations.

2.4.1 Probing gluon polarization (from here on we'll need to insert things from Steve Vigdor below!)

As follows from Table 1, gluon polarization can be probed in a variety of ways at RHIC. This is important, since it will important cross-checks testing the consistency of the various measurements and of the theoretical framework.

Prompt-photon production. The "gold-plated" channel at RHIC is prompt-photon production $pp \to \gamma X$ which is largely driven by the Compton process $qg \to \gamma q$ and is a particularly probe clean thanks to the photon final state. We emphasize again that from the results shown in the preceding section, Fig. **??**, we know that NLO theory provides a good description of the unpolarized cross section for $pp \to \gamma X$ already measured at RHIC, which gives confidence that NLO predictions for the double-spin asymmetry for $pp \to \gamma X$ are realistic as well.

Figure 8 shows such theoretical NLO calculations for A_{LL}^{γ} at RHIC, for $\sqrt{S} = 200$ GeV. An isolation cut on the photon has been imposed. The key point is now to assess the sensitivity to gluon polarization, Δg. To do this, we choose the sets of polarized parton distributions by [**?**] that we already introduced in Figure **??**. As we discussed there, the shaded bands represent the "1-σ" uncertainties with which we currently know the densities from deeply-inelastic scattering. The authors of [**?**] provide parameterizations of parton density sets that span these bands, which are ideally suited for estimating the sensitivities and expected improvements from RHIC. For the reader's convenience, we show in the left part of Fig. 8 again the uncertainty in the polarized gluon density, which turns out to be the clearly dominant factor here. The shaded band translates into the band shown for A_{LL}^{γ} on the right-hand-side, which would then represent the uncertainty related to Δg which we would *currently* have in predictions of that spin asymmetry. For further comparison, we also show a theoretical prediction based on a very negative gluon polarization function [**?**], which is currently only marginally excluded by the DIS data. The error bars given in the figure are projections for statistical errors achievable at RHIC with polarization $P = 0.7$ and integrated luminosity $\mathcal{L} = 100$/pb. Figure 9 shows similar results, but at $\sqrt{S} = 500$ GeV, and with expected errors for $P = 0.7$ and $\mathcal{L} = 300$/pb. It is evident

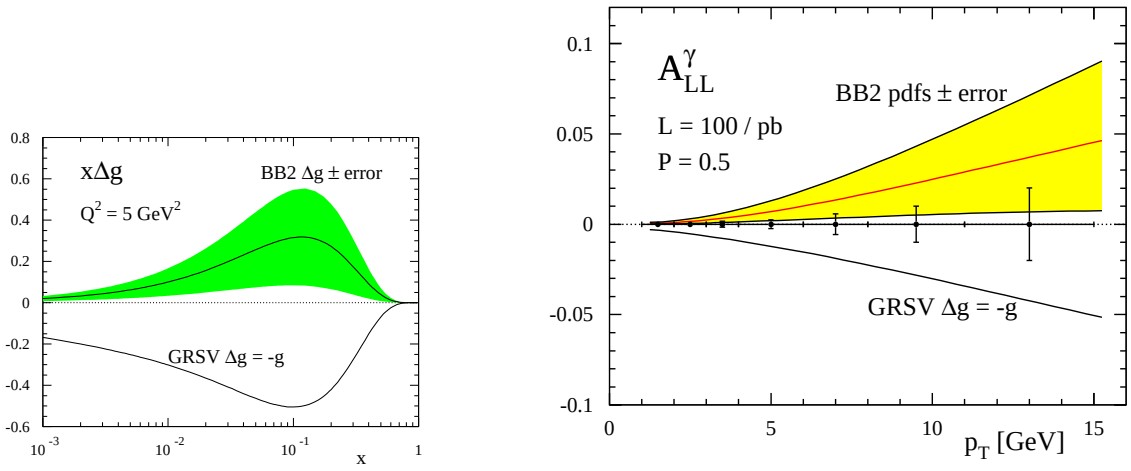

Figure 8: Left: current uncertainty in $\Delta g(x)$ from polarized DIS, as given by the set of polarized parton distributions of [**?**]. Right: range of spin asymmetries A_{LL} for prompt photon production corresponding to that uncertainty . Expected statistical error bars at RHIC for $\sqrt{S} = 200$ GeV are shown for $P = 70\%$ and $\mathcal{L} = 100$/pb. The calculations have been performed for the acceptance of the Phenix detector.

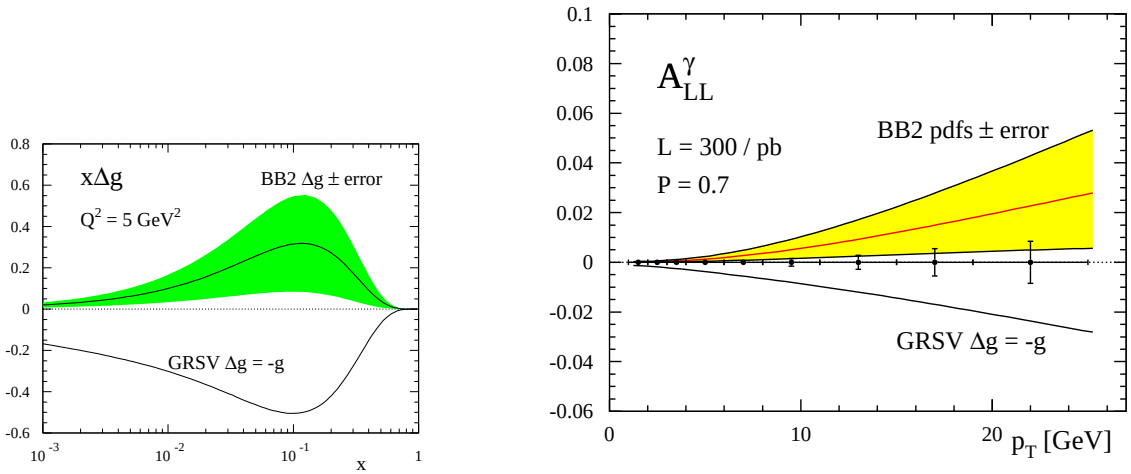

Figure 9: Same as Fig. 8, but for $\sqrt{S} = 500$ GeV.

that RHIC measurements will significantly reduce the uncertainty in Δg through prompt photon measurements alone.

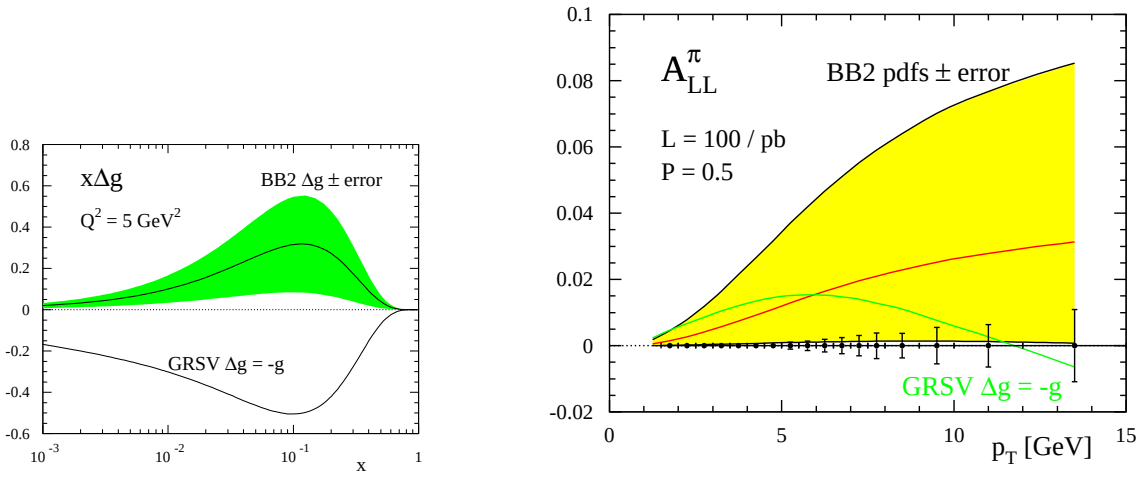

Figure 10: Same as Fig. 8, but for $pp \to \pi^0 X$ at central rapidities.

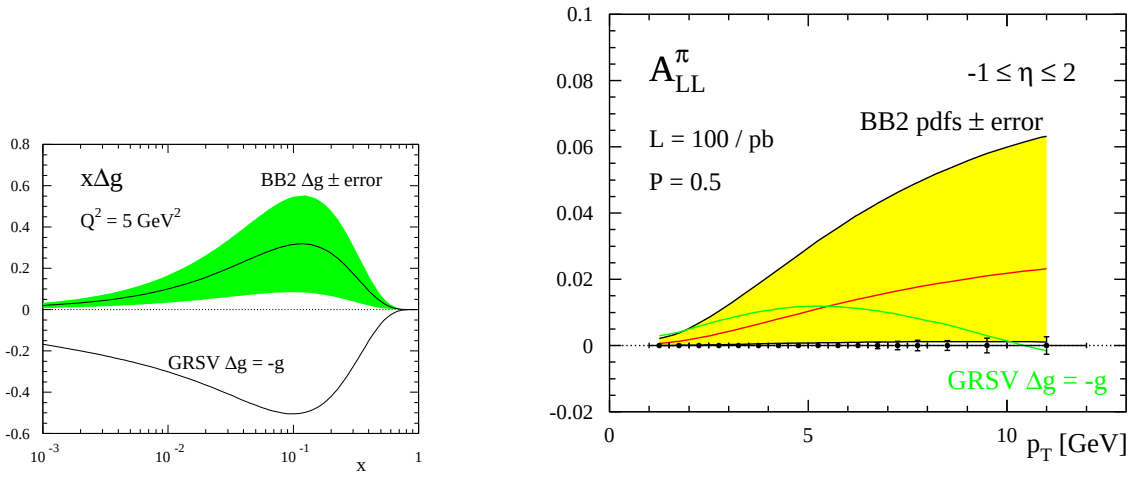

Figure 11: Same as Fig. 8, but for $pp \to \pi^0 X$ at slightly forward rapidities, $1 \leq \eta \leq 2$.

High-p_T pion and jet production. Hadrons and jets are very copiously produced in pp collisions, which results in very small statistical uncertainties of the spin asymmetries.

(Anti)quarks from W production (Bernd) 1. Naive pQCD picture/expectation of generation of QCD sea to be flavor symmetric (g -¿ qqbar)

2. Unpolarized result on u/d: flavor asymmetry in unpolarized sector

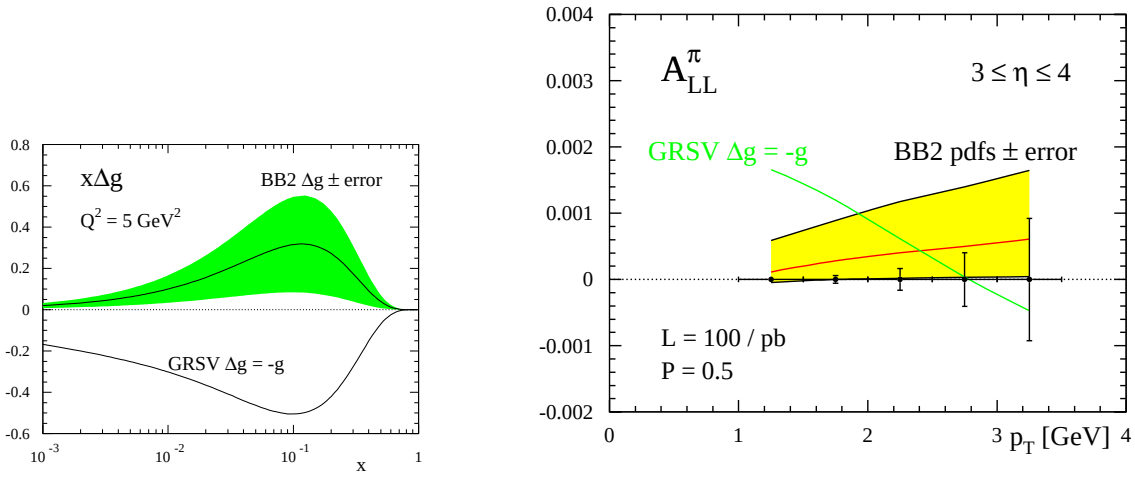

Figure 12: Same as Fig. 8, but for $pp \to \pi^0 X$ at very forward rapidities, $3 \leq \eta \leq 4$.

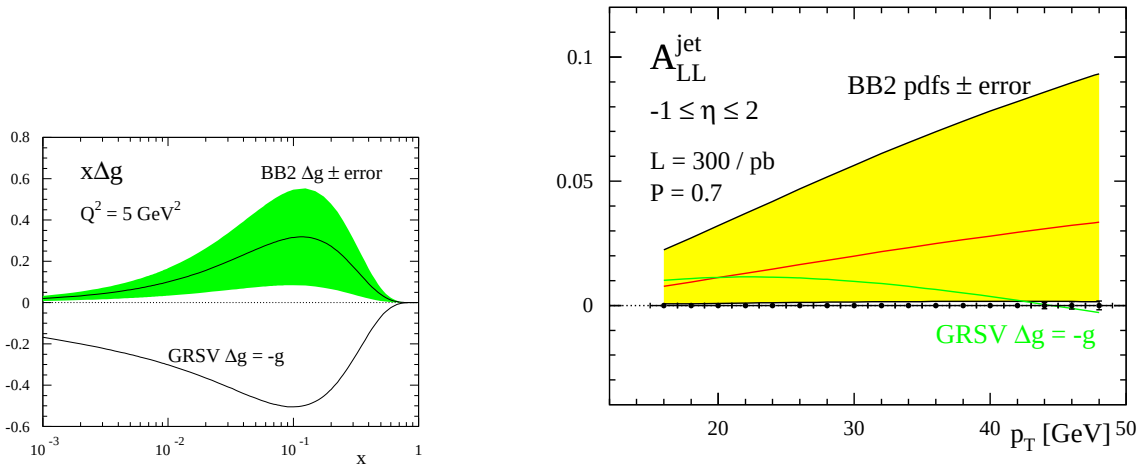

Figure 13: Same as Fig. 8, but for $pp \to \mathrm{jet}X$ at rapidities, $1 \leq \eta \leq 2$ and $\sqrt{S} = 500$ GeV.

3. Non-perturbative QCD approach to account for this effect and discuss expectation for polarized case

4. Means to probe the flavor structure in the polarized sector:

a. DIS (e.g. SMC): Discuss limitations

b. RHIC SPIN case through W production (Figure 1: Feynman graph)

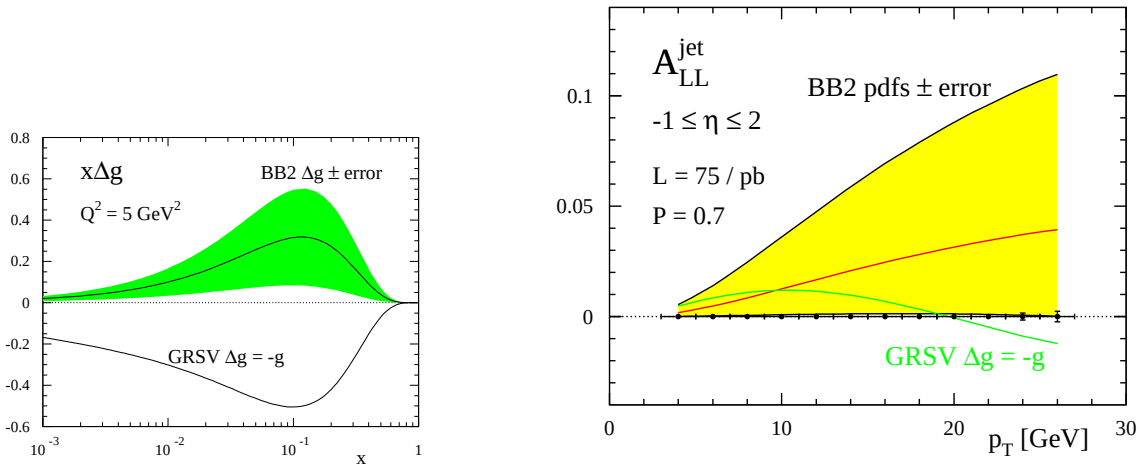

Figure 14: Same as Fig. 13, but for $\sqrt{S} = 200$ GeV.

5. Discuss reconstruction of W with RHIC detectors (non-hermetic) and argue for leptonic asymmetries (RHICBOS) besides reconstruction of W rapidity. Stress forward direction

6. Show expectation for STAR (Figure 2) / PHENIX (Figure 3)

7. Summarize importance of this measurement in QCD: QCD sea production mechanism

2.5 RHIC Spin Report for DOE: Outline of Gluon Section 2.3.2 (by S. Vigdor)

(each major heading represents 1 paragraph; some of the figures will likely appear in other sections of the report)

A. Experimental approaches to determining gluon helicity preferences in p+p

1. Advantages of p+p: direct gluon involvement at LO; sizable pQCD spin sensitivity via ALL. 2. Goals: improve statistical precision on (g(x) by at least a factor 2 vis--vis DIS analyses, for x 0.1; reduce interpretation uncertainties via direct sensitivity; extend measurements to as low x as possible, to permit constraint on integral (g. 3. Demonstrate robustness of (g(x) extraction, evaluate interpretation uncertainties by comparing: results for different channels, with differing experimental/ interpretation issues; results for same x range probed at different pT (evolution sensitivity); results with different constraints on flavor and x-range of colliding partner parton; quark polarizations extracted from p+p with those from DIS. 4. Figure: LO Feynman diagrams relevant to jet, photon and heavy flavor production.

B. Abundant probes: inclusive jet and pion ALL

1. Advantages: large cross sections; NLO success for (0 cross sections; significant (g sensitivity. 2. Disadvantages: competition among LO subprocesses; combination of linear and quadratic sensitivity to (g, and pT-dependent dilution from qq contributions; sensitivity to fragmentation functions and convolution over significant range of partonic pT scales; possible jet trigger biases; averaging over substantial x-range. 3. (0 and jet reconstruction efficiencies in PHENIX, STAR 4. Projected timeline and achievable uncertainties, compared to models consistent with DIS database. Figures: PHENIX (0, ALL results and projections; STAR jet ALL projections for run 5.

C. Dijet and dihadron correlations

1. Measure ALL as function of pT and ((: exploit unpolarized PDF differences and quark vs. gluon fragmentation differences to vary partonic subprocess sensitivities in controlled way. 2. Figure: from Les, to indicate subprocess sensitivity for different rapidity intervals in di-hadron measurements (?)

D. Inclusive direct photon production

1. Advantages: dominance of QCD Compton at LO; direct measurement of pT for partonic subprocess (modulo kT uncertainties). 2. Interpretation issues: NLO difficulties for cross sections; fragmentation photon contributions, and the effect of experimentally achievable isolation cuts on analysis; how low in pT is analysis robust? 3. Experimental issues: low cross section; (0 background suppression; need to develop isolation cuts in association with theorists; (reconstruction efficiency. 4. Figures: (ID from PHENIX; projected ALL uncertainties for 200 pb-1 delivered, 70

E. Photon-jet and photon-leading hadron coincidences

1. Advantages: comparable statistical sensitivity to inclusive photon; event-by-event constraints on colliding parton kinematics permit systematic study of sensitivity to cuts, variation of asymmetries with x of collision partner, etc. 2. Disadvantages: jet reconstruction may impose more stringent low-end limit than photon detection on pT extent of useful measurements. 3. Projected timeline and achievable uncertainties and x-range compared to DIS, COMPASS, SMC, HERMES. 4. Figure: STAR simulations of ALL, x(g(x) LO extraction, scaled for 200 pb-1 delivered at 200 GeV, for estimated (reconstruction efficiency and for pT ¿ 5 GeV/c.

F. Heavy flavor production

1. Features: independent channel to cross-check results; emphasizes g-g fusion, quadratic sensitivity to (g; small x accessible via forward lepton detection. 2. Interpretation issues: how well understood are charm production cross sections? How cleanly can different contributions be separated in inclusive lepton channels? 3. Experimental issues: can displaced vertex cut with improved inner tracking improve heavy flavor ID significantly without too much sacrifice in yield? 4. Figure: PHENIX projection of open charm ALL.

G. Importance of measurements at 2 energies

1. Approaches to extending to lower x: raising energy; increasing forward coverage (subject to pT limit for interpretability); need to get beyond maximum in x(g(x) to constrain integral (g. 2. Need for 200 GeV: gives overlap with COMPASS, etc. sensitivity; constrains x(g(x) where

uncertainties from DIS analysis are largest. 3. Need for 500 GeV: permits sensitivity down to xg 0.01; permits test of evolution and robustness of analysis, by comparison of results at similar x, different pT. 4. Figure: Projection of STAR (g(x)/g(x) uncertainties achievable with 200 pb-1 (delivered) at 200 GeV and 500 pb-1 (delivered) at 500 GeV, compared to models consistent with DIS database, COMPASS achieved & projected, etc.

2.6 Transverse spin structure

2.6.1 Introduction (Jianwei)

With the proton spin (S) transversely polarized with respect to its momentum (P) or the collision axis, new asymmetries, in particular, the single spin asymmetries (SSA), which are otherwise forbidden in QCD, are theoretically allowed. Measurements of transverse spin asymmetries can not only provide additional information on parton's helicity distributions inside a proton, but also probe the proton structure that can never be reached by the observables of longitudinal spin asymmetries.

Parton distributions $f(x)$ and corresponding helicity distributions $\Delta f(x)$ provide excellent microscopic information on parton helicity structure inside a proton. However, complete parton helicity structure requires our knowledge of a novel helicity flip chiral-odd quark distribution - known as the transversity distribution $\delta q(x)$, which can only be measured in terms of transverse spin asymmetries because of its helicity flip nature. Transversity distribution $\delta q(x)$ is as fundamental as $f(x)$ and $\Delta f(x)$ in QCD. But, it is not completely independent because of the Soffer's Inequality,

$$|2\,\delta q(x)| \leq q(x) + \Delta q(x)\,,$$

which is valid for each quark flavor q. Independent measurements of $\delta q(x)$ and $\Delta q(x)$ can help putting limits on each other. The size of $\delta q(x)$ is crucial in generating double transverse-spin asymmetries, A_{TT}, as well as single transverse-spin asymmetries, A_N.

Single longitudinal-spin asymmetries for single particle inclusive production vanish because of parity and time-reversal invariance. However, significant single transverse-spin asymmetries, A_N, of ten or more percent of the unpolarized cross sections, were recorded by Fermilab E704 experiment in the beam fragmentation region of hadronic π production at p_T as large as GeV [32]. Since then, nonvanishing single transverse-spin asymmetries have been observed in lower energy hadronic collisions [33] and semi-inclusive lepton-hadron deeply inelastic scattering (SIDIS) [34, 35], as well as, in much high energy pp collisions at RHIC [36].

Theoretically, on the other hand, it was pointed out long ago [31] that perturbative QCD calculation at leading power in collinear factorization formalism predicts vanishing single transverse-spin asymmetries, A_N, in single hadron inclusive production at high p_T. Because of Lorentz invariance of QCD, we need at least four vectors including the spin vector to construct a physically observed SSA. With a proton spin vector S not parallel to its momentum, a hadron level SSA can be constructed to be proportional to $\epsilon_{\mu\nu\alpha\beta}S^\mu P_A^\nu P_B^\alpha p^\beta$ with beam momenta, P_A and P_B, and observed particle momentum p. However, inclusive production of a high p_T single parton in collision between two massless collinear partons does not have enough vectors to construct a parton level SSA. Additional transverse direction from parton's k_T or physical polarization of an

extra gluon is necessary to connect to the spin vector S for generating the SSA. Therefore, measuring single transverse-spin asymmetries in hard collisions directly probe partons' transverse motion as well as multiparton correlations inside a hadron. Single transverse-spin asymmetries generated by parton's transverse motion in a transversely polarized hadron is characterized by the Sivers function [37]. Single transverse-spin asymmetries can be also generated by the Collins' fragmentation function from a polarized parton [38]. Within the collinear factorization formalism, single transverse-spin asymmetries are consequences of coherent multiparton interactions characterized by high twist matrix elements, and the rising x_F dependence of the asymmetries is a natural result of the short distance dynamics [40, 41].

QCD factorization is necessary for reliable calculations of single transverse-spin asymmetries in hadronic collisions. For extracting Sivers function and Collins function, which are sensitive to the information of partons' intrinsic transverse momenta, a k_T factorization formalism is required [39]. Since dynamics at parton's typical intrinsic k_T is nonperturbative, additional hard scale, such as Q^2 in SIDIS, is necessary for reliable perturbative QCD calculations of single transverse-spin asymmetries at $p_T \sim \mathcal{O}(k_T)$ [**?**]. Since p_T is only large momentum scale in inclusive single hadron production in hadronic collisions and QCD factorization fails when $p_T \sim \mathcal{O}(k_T)$, single transverse-spin asymmetries at large enough p_T are probes of multiparton correlations (or high twist matrix elements), which are as fundamental as parton helicity distributions [40]. The leading twist-3 quark gluon correlation function responsible for the high p_T and x_F single transverse-spin asymmetries gives a measurement of typical size of color Lorentz force inside polarized hadron [40]. When p_T decreases, nonperturbative physics at the scale of intrinsic k_T becomes more relevant the asymmetries should be roughly proportional to the dimensionless coefficient: $p_T M_1/(p_T^2 + M_2^2)$ where $M_1 \sim M_2$ are typical nonperturbative hadronic scales (e.g., gluon condensate scale, or diquark mass in Ref. [**?**]). Measurement of single transverse-spin asymmetries as a function of p_T is an excellent probe of both perturbative and nonperturbative QCD dynamics.

• history, previous A_N measurements (**Les,Matthias,Akio**)
- Description of E704[32] and why it was a surprise[31]
- Theory developments since then: Sivers[37], Collins[38] and Boer[39] with k_T factorization. Also describe collinear twist-3 approach[40, 41]
- Predictions for $\sqrt{s} = 200$ GeV[42, 43, 40, 41] and more recent developments[44]
- More recent pp experiments[33] and SDIS experiments[34, 35]
- RHIC results[36], A_N at large x_F stays at an order larger $\sqrt{s}$
- Need cross section at $\sqrt{s} = 200$ GeV arguments? Note that there is separate section for it
- Fig15 shows A_N from 3 RHIC experiments

• mapping A_N in x_F and p_T plane (**Les,Matthias,Akio**)
- Mapping A_N in x_F and pT plane
- pQCD prediction of $1/p_T$ dependence and importance of measurement, need for more data
- Interests in very large x_F[45] and soffer bounds[46]
- Negative x_F and sensitivity to gluon Siver's functions[44][36]
- Global fits with pp data and SDIS(?)
- L and P requirements
- Fig16 shows projection for A_N as function of p_T for STAR

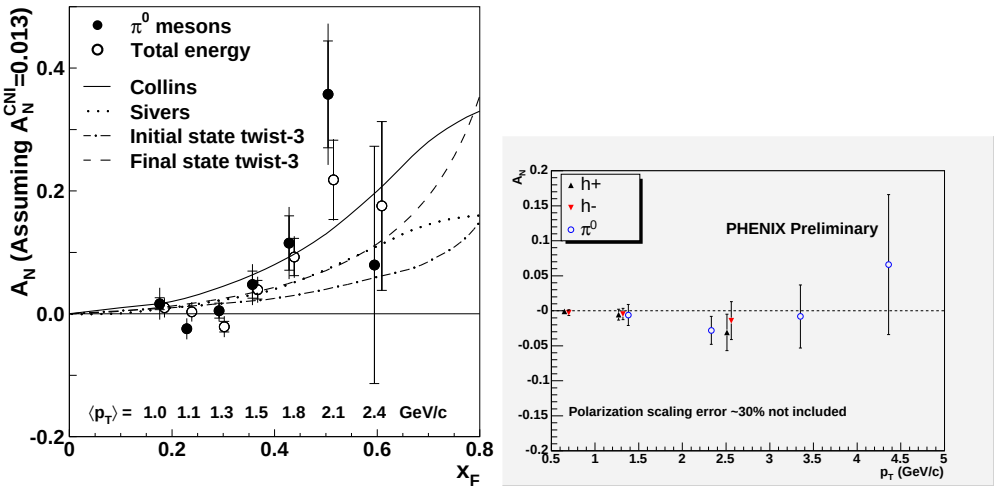

Figure 15: Single Spin asymmetry A_N for π^0 production at STAR (Left), π^- production at BRAHMS (Middle) as function of x_F at forward rapidity. A_N for $\pi^\pm$ production from PHENIX (Right) as function of p_T at mid-rapidity.

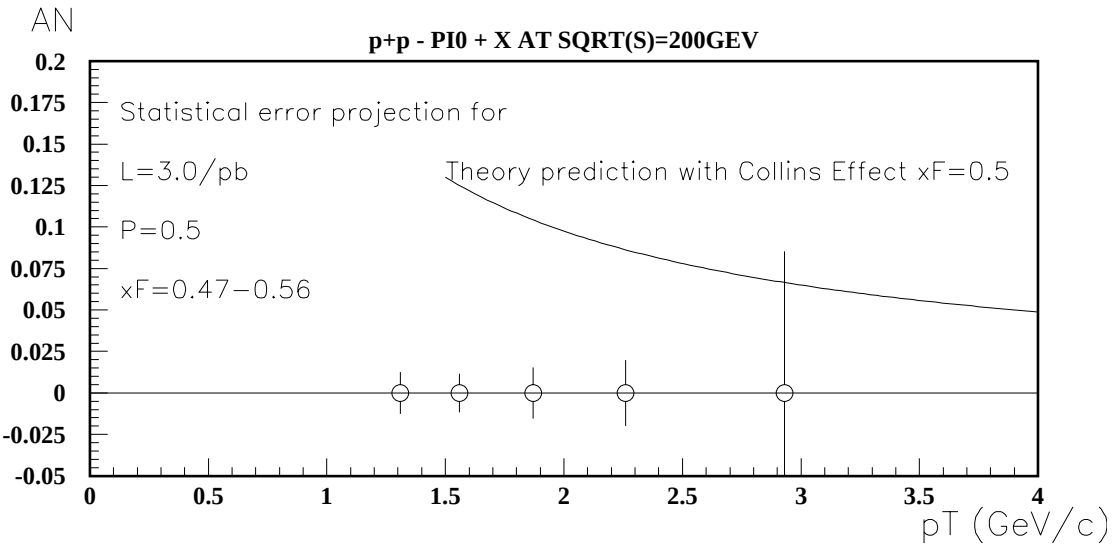

Figure 16: Statistical error projection for A_N as function of p_T for π^0 production at STAR. A theory prediction for Collins effect (need citation!) for $x_F = 0.5$ is also shown.

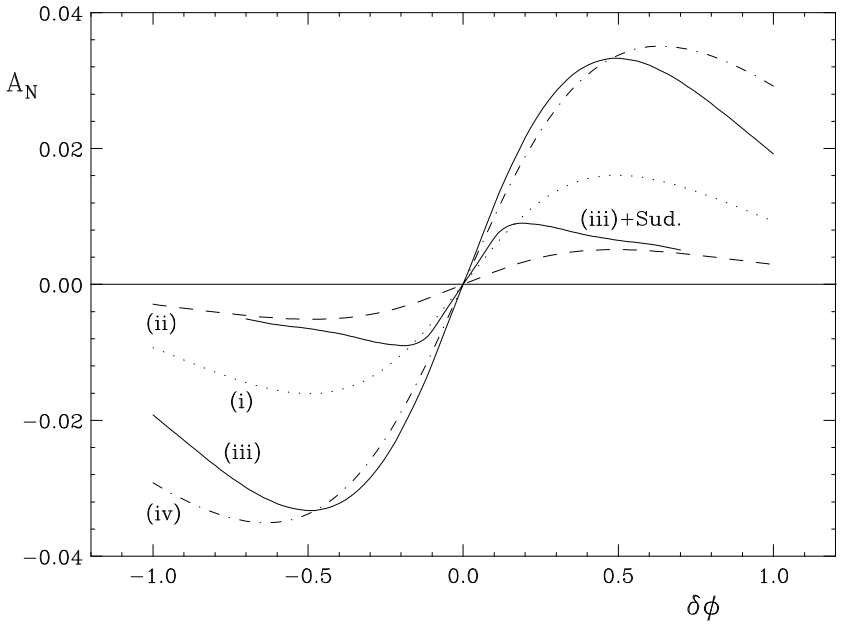

Figure 17: Predictions for the spin asymmetry AN for back-to-back dijet production at $sqrts = 200$ GeV, for various different models for the gluon Sivers function. The solid line marked as "(iii)+Sud" shows the impact of leading logarithmic Sudakov effects on the asymmetry for model (iii)[47].

• Away side di-jet/hadron for Sivers (**Les,Matthias,Akio**)

- Need to go beyond inclusive measurement to disentangle different effects (except A_N for "inclusive" jet at forward)
- Di-jet measurement for gluon sivers measurement for non-power supressed/direct k_T sensitivity[47]
- Di-hadron measurements at forward $\rightarrow$ to access large x quark sivers?
- Connection to parton motion/orbital angular momentum/GPD, "modified" universality, etc? (maybe in theory section?)
- L and P requirements
- Fig17 shows theory prediction for di-jet A_N (no exp error estimate yet)

• Near side di-hadron for Collins (**Les,Matthias,Akio**)

- Transversity, last unmeasured leading twist quark PDF, no gluon transversity, Lattice results(maybe in theory section?)
- Collins and Interference FF[38], and describe models[48]
- How to measure - azimuthal correlation between hadrons within a jet
- Getting FF from e+e- to turn into Transversity measurement[49][50]
- Measuring over large p_T and rapidity range to see x_{BJ} dependence of transversity
- L and P requirements
- Fig(yet coming): transversity measurement at PHENIX with 30/pb and P=0.5 by Matthias

• A_{TT}(jet, photon, DY) and beyond (**Les,Matthias,Akio**)

- This measures $\delta q \times \delta qbar$ [51], no need for FF, but small
- DY need more luminosity[52]
- Transversity from J/psi[53]
- Sivers from D mesons[54]

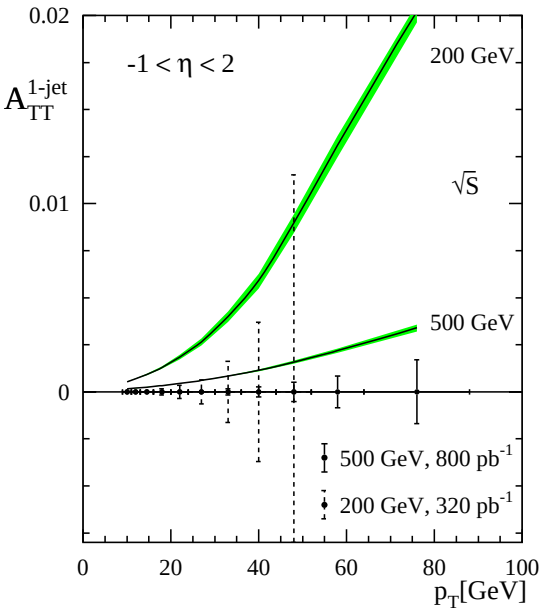

Figure 18: Maximally possible A_{TT} for single-inclusive jet production at $sqrts = 200$ and 500 GeV as a function of pT. Jet rapidities are integrated over $-1 < \eta < 2$. The shaded bands represent thetheoretical uncertainty in A_{TT} estimated by varing scale by factor 2. Also indicated as error bars is the expected statistical accuracy with design luminosity of the RHIC [51].

- L and P requirements
- Fig18 shows maximum A_{TT}^{jet} and projection for STAR acceptance

• assess what requirements would be for key measurements here, and how they would compare to longitudinal running(**Les,Matthias,Akio**)
- 3/pb, p=0.5 : Inclusve
- 10/pb, p=0.5 : Sivers from di-jet/hadron
- 30/pb, P=0.5 : Transversity measurement from di-hadron correlations within a jet
- 100/pb, P=0.7 : A_{TT} of jet/hadron
- 1000/pb, P=1.2 : DY
- 1/3 to 1/4 of beam time, and we'll have intermediat physics as LP develops.
- STAR and PHENIX are independent for choice of long and trans
- Most of measurements prefers $\sqrt{s} = 200$ GeV

2.7 "What else is going on in the world"

• briefly discuss current efforts in DIS and their expected results & timelines (**Ernst, Akio**)

2.8 Soft interactions of polarized high energy protons (L. Trueman)

• Historically, when high energy hadronic beams first became available, near-forward elastic scattering was at the center of attention, largely because the optical theorem encodes the sum of cross sections into the forward amplitude. With the advent of QCD attention turned to high energy primarily as a source of rare events with large momentum transfer: short-distance processes. Short-distance processes are only part of the picture, however, even for high-energy hadronic collisions. A large and growing community of theorists and experimentalists is making strides toward understanding what makes up the bulk of the high-energy cross section in proton-proton collisions: low-momentum transfer elastic and diffractive scattering. The theory of near-forward elastic scattering at very high energy predates QCD, of course, and not long before the gauge theory revolution, Regge theory provided the predominant approach to this kinematic domain. It was displaced by QCD in the foreground of theoretical interest, in part because there are few results in Regge theory that can be derived from first principles in quantum field theory. On the other hand, Regge theory remains a valuable tool to organize an important kinematic region where it is most difficult to get answers from first-principles QCD: long distances and low momentum transfers.
• Conceptually, the simplest measurement is the total cross section $\sigma_{\rm tot}$, which is given by the imaginary part of the forward spin-independent amplitude. Closely related is $\rho(s)$, the ratio of the real-to-imaginary parts of the amplitude at $t = 0$. The value of the slope of the forward amplitude B is also very useful to know. All of these quantities have spin dependent variants for both transverse and longitudinally polarized protons. A little information is known about this spin dependence, but not much, and the information would be very useful in determining the Regge dynamics.
• For the differential cross section $\frac{d\sigma(s,t)}{dt}$ we can roughly divide the near-forward elastic scattering into four fairly well-defined regions, toward increasing $-t$: the Coulomb interference region, the diffractive (or pomeron exchange) region, the "dip" region, and the beginning of the perturbative region. The physics of each of these regions is different and the spin-dependence can be used as a tool for analyzing these different dynamics.
• In the very forward region, the nuclear and electromagnetic amplitudes are of comparable magnitude, resulting in a small but significant maximum in the single transverse spin asymmetry A_N making it a useful quantity for polarimetry. First measurements of A_N have been made RHIC with colliding polarized beams and also with a polarized proton gas jet target, with some very precise and interesting results already reported. Successful applications to polarimetry have been made at the same time.
• At somewhat larger $-t$, the spin dependent asymmetries are sensitive probes of the various Regge exchanges which contribute the hadronic amplitudes. Of special interest is the C-odd, three-gluon exchange giving rise to the putative "odderon" which contributes to the observed difference between pp and $\bar{p}p$ scattering in the dip region. It has a very distinctive interference pattern with the pomeron at small $-t$, observable in both A_N and the double transverse spin asymmetry A_{NN}. More generally, the spin-dependence of most Reggeons is not known at all, except in the CNI region where first information on this is emerging from the early RHIC polarized proton runs. This knowlege is crucial to understanding the fundamental nature of the various Reggeons, in particular the pomeron.
• Passing through the dip region toward the perturbative QCD region, a steep exponential fall with momentum transfer, characteristic of pomeron exchange matches on to an approximate t^{-8} dependence at larger $-t$ in the unpolarized cross sections. The latter has a natural interpretation in terms of three vector exchanges between pairs of valence quarks. Whether these individual

scatterings should be thought of as single gluons, or as (at least in part) perturbative exchanges in color-singlet configurations remains to be seen. This profile is fairly stable with energy, even as the details of its shape change. The observation of a stable profile in polarized elastic scattering at RHIC would surely initiate a new class of theoretical investigations.

• The dramatic spin dependence of proton-proton elastic scattering at moderate $-t$ observed in the Argonne and BNL experiments of twenty years ago remains an outstanding puzzle. Sensitive measurements of the same quantities as a function of energy at RHIC could be the key missing piece.

• Beyond the quantities A_N and A_{NN} there are several other double spin asymmetries which could be measured with the use of spin rotators: A_{LL}, A_{SS} and A_{SL}. These are likely to be small and difficult to measure, but their values would put strong model-independent constraints on the pp amplitudes. They could, in principle, be used to provide a self-calibrating polarimeter.

• A complete understanding of the Regge theory of pp scattering requires the knowledge of the isospin of the various Regge contributions. This can be obtained by using beams or fixed targets of nucleii to scatter on the polarized proton beam. Significant success has already been made using a carbon filaments target and this will be pursued in the future. Deuterons and He^3 nuclei, either polarized or unpolarized, should also be considered as ways to get at the pn scattering spin dependence.

• Inelastic diffractive scattering is closely related soft physics that goes beyond elastic scattering. This includes exclusive small angle resonance production and various rapidity gap measurements. These have been carried out for unpolarized protons and are interpreted in terms of the scattering of the pomeron on the proton or the pomeron on another pomeron ("double pomeron exchange") depending on the configuration. This last has been argued to provide a special source of exotic mesons and, in particular, glueballs. The systematic extension to the spin dependence is certain to help our understanding of these processes; for example, how does the ϕ dependence of the rapidity gaps depend on the spin state of the proton? Much theoretical work remains to be done in this area in order to optimize the kinematics and understand the signatures.

2.9 Future plans/ideas at RHIC

2.9.1 Physics beyond the Standard Model (M.J.Tannenbaum)

At RHIC, the standard model parity violating effects are large. In inclusive single jet production, the leading strong interaction process, the two-spin parity violating asymmetry, A_{LL}^{PV}, due to the interference of gluon and W exchange is $\sim 1\%$ at $\sqrt{s} = 500$ GeV (see Fig. 19 SM). Of course, a more spectacular effect at RHIC concerns the direct production of the Weak Bosons, $W^{\pm}$ and Z^0, visible through their di-jet or di-lepton decay. The peak from $W \rightarrow$ Jets is evident in Fig. 19. Flavor-identified structure function measurements using $W^{\pm}$ production are discussed elsewhere

Figure 19: Prediction [58] for A_{LL}^{PV} in inclusive jet production at RHIC. Solid curve is standard model (SM), with error bars corresponding to sensitivity with $L = 0.80$ fb^{-1} integrated luminosity. Dot-dash curves are contact model of quark compositeness with $\Lambda_c = 1.6$ TeV.

in this document. Here we concentrate on the physics beyond the standard model that is opened up by searches for parity violating effects at RHIC. A typical example of such a possibility is

quark compositeness or substructure [55]. Composite models of quarks and leptons [56] generally violate parity, since the scale of compositeness $\Lambda_c \gg M_W$. Without the Parity Violating Asymmetry (PVA) handle, detectors at the Tevatron are limited to searching for substructure by deviations of jet production from QCD predictions at large values of p_T. It is difficult to prove that a small deviation is really due to something new. However a few % parity-violation effect would be **a clear indication of new physics**. The experimental limit is presently [57] $\Lambda_c \cong 1.6$ TeV. The estimate of sensitivity to compositeness at RHIC [58] with this value of Λ_c is shown on Fig. 19. The error bars shown on the standard model correspond to $L = 0.80$ fb^{-1} integrated luminosity. Structure function uncertainties can be calibrated out using the PVA in $W \rightarrow$ Jet (inclusive) which is clearly visible on the plot. The limits of sensitivity for Λ_c in the contact model of quark compositeness [59] are tabulated in Table 2 for the standard $L \sim 1$ fb^{-1} integrated luminosity of the original RHIC-spin run plan. The limits increase siginificantly with factors of 10

$\sqrt{s}$ GeV	L(fb^{-1})	Λ_c (TeV)
500	1	3.3
500	10	5.5
500	100	7.5
650	1	3.8
650	10	6.3
650	100	8.8

Table 2: Limits on $\Lambda(\epsilon = -1)$ at 95% CL, P=0.7, $\Delta\eta = 1$, 10% systematic error in Asymmetry [59].

and 100 increase in luminosity (but for this reaction, are not much improved with increasing c.m. energy). For comparison, at the Tevatron, sensitivity is $\Lambda_c \sim 4$ TeV for L =2 fb^{-1} (Run II) and 5 TeV for 30 fb^{-1} (Run III) and $\Lambda_c \sim$ 20-30 TeV at the LHC for $L = 10 - 100$ fb^{-1}. Of course, even if an anomaly were found at either the Tevatron or the LHC, only RHIC will be able to provide polarization information on the anomaly to determine what its chiral properties are and whether it is a new interaction, a supersymmetric particle, or anything with a non-standard-model spin signature.

2.9.2 Physics beyond the Standard Model (V. L. Rykov and K. Sudoh)

RHIC-Spin potential for uncovering new physics beyond the Standard Model (SM) has been explored in a number of last decade publications. Our purpose in this section is to illustrate this new potentiality by means of a few specific examples.

The non-SM modifications of parity-violating helicity asymmetry $A_L = (\sigma^+ - \sigma^-)/(\sigma^+ + \sigma^-)$ for one-jet production in collisions of the longitudinally polarized protons at unpolarized has been studied in Refs. [60, 61]. In the A_L definition above, σ^+ and σ^- are for the cross sections* with the positive and negative helicities of the initial protons, respectively. In the SM, inclusive jet production is dominated by the pure QCD gg, gq, and qq scattering which conserve a parity. However the existence of electroweak interactions through the $W^\pm$ and Z gauge bosons gives

*Or differential cross sections.

a small contribution to A_L. Consequently, the A_L is expected to be nonzero from the QCD-electroweak interference (as shown in Fig. 20). Additionally, a small peak near $E_T = M_{W,Z}/2$ is seen, which is the main signature of the purely electroweak contribution. The existence of new parity-violating interactions could lead to large modifications of this SM prediction [63].

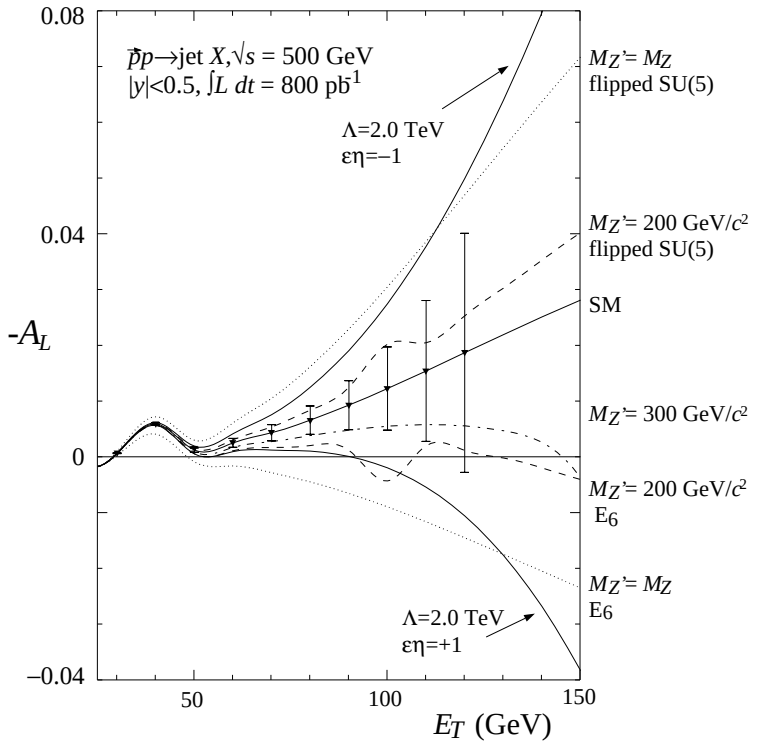

Figure 20: A_L, for one-jet inclusive production in $\vec{p}p$ collisions versus transverse energy, for $\sqrt{s} = 500$ GeV. The solid curve with error bars represents the SM expectations. The error bars show the sensitivity at RHIC for 800 pb^{-1}, for the STAR detector. The other solid curves, labeled by the product of $\epsilon\eta$, correspond to the contact interaction at $\Lambda = 2$ TeV [60]. The dashed and dotted curves correspond to different leptophobic Z' models. The calculations are at the leading order.

The modifications due to the presense of quark substructure have been analyzed in Ref. [60] in the framework of an effective Lagrangian approach. Such effects are generally realized as quantum effects of new physics where new heavy particles are considered to be decoupled. The non-SM Lagrangian could be represented in terms of new quark-quark contact interactions[†] under the form:

$$\mathcal{L}_{qqqq} = \epsilon\frac{g^2}{8\Lambda^2}\overline{\Psi}\gamma_\mu(1-\eta\gamma_5)\Psi\cdot\overline{\Psi}\gamma^\mu(1-\eta\gamma_5)\Psi \quad , \tag{7}$$

where Ψ is a quark doublet, g is a non-standard coupling, Λ is a compositeness scale, and $\epsilon = \pm 1$. If parity is maximally violated, $\eta = \pm 1$. Fig. 20 shows how the SM prediction will be affected by such a new interaction, assuming $\Lambda = 2$ TeV, which is close to the present limit obtained for example by the DØ experiment at the Tevatron [64]. The statistical errors shown are for RHIC luminosity of 800 pb^{-1}, and for the jets with rapidity $|y| < 0.5$, and include measuring A_L using

[†] It is assumed here that only quarks are composite.

each beam, summing over the spin states of the other beam. Due to the parity-violating signal's sensitivity to new physics, RHIC is surprisingly sensitive to quark substructure at the ∼2-TeV scale and is competitive with the Tevatron, despite the different energy range of these machines. Indeed, a parity-violating signal beyond the SM at RHIC would definitely indicate the presence of new physics [63].

RHIC-Spin would also be sensitive to possible new neutral gauge bosons [61, 62]. A class of models, called leptophobic Z', is poorly constrained up to now. Such models appear naturally in several string-derived models [65] (non-supersymmetric models may be also constructed [66]). In addition, in the framework of supersymmetric models with an additional Abelian $U(1)'$ gauge, it has been shown [67] that the Z' boson could appear with a relatively low mass ($M_Z \leq M_{Z'} \leq$ 1 TeV) and a mixing angle with the standard Z close to zero. The effects of different representative models are also shown in Fig. 20 (see Ref. [61] for details). RHIC covers some regions of parameters space of the different models that are unconstrained by present and forthcoming experiments, and RHIC would also uniquely obtain information on the chiral structure of the new interaction. In Ref. [62], it has been suggested to extend this study to the collisions of polarized neutrons, which could be performed with colliding at RHIC polarized ^3He nuclei [68]. The authors argue that, in case of a discovery, a compilation of the information coming from both polarized $\vec{p}\vec{p}$ and $\vec{n}\vec{n}$ collisions should constrain the number of Higgs doublets and the presence or absence of trilinear fermion mass terms in the underlying model of new physics.

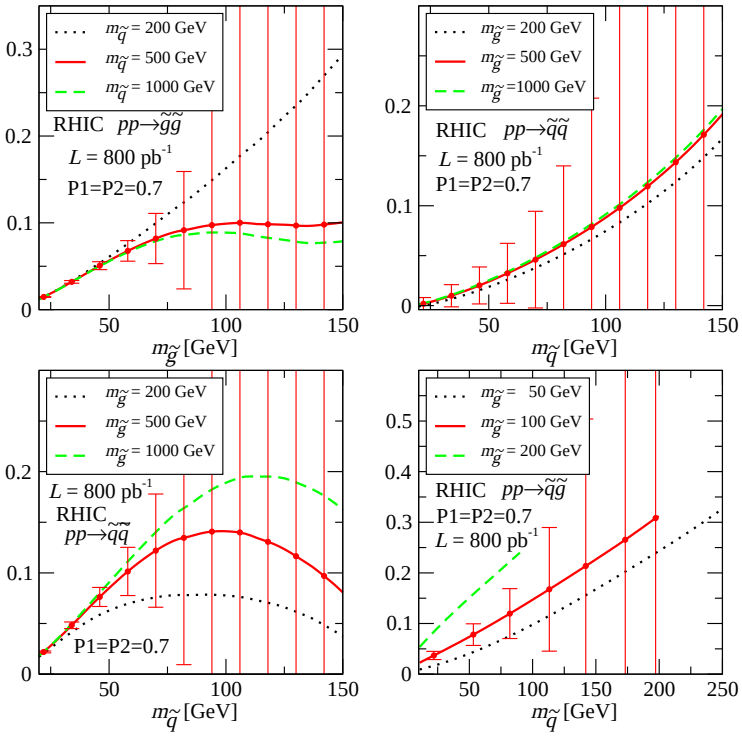

Figure 21: The leading order A_L predictions for sparticle production at RHIC (see Ref. [69] for details). Using the full-scale high-energy physics detector of $\sim 4\pi$ acceptance, similar to, for example, the one proposed in Ref. [71], with the capability of measuring multi–jet events and missing transverse energy is assumed.

The study of the production cross sections for squarks and gluinos in collisions of longitudinally polarized hadrons has been undertaken in Ref. [69]. The resulting asymmetries are

evaluated for the polarized proton collider RHIC, as well as for hypothetical polarized options of the Tevatron and the LHC. These asymmetries turned out to be sizable over a wide range of supersymmetric particle masses. Once supersymmetric particles are discovered in unpolarized collisions, a measurement of the spin asymmetries would thus potentially help to establish the properties of the newly discovered particles and open a window to detailed sparticle spectroscopy at future polarized colliders. Although non-observation of squark and gluino signatures at the Tevatron thus turns into the stringent limits on the squark and gluino masses in a frame of MSSM[‡] [70]: $m_{\tilde{q}} > 250$ GeV, $m_{\tilde{g}} > 195$ GeV, these limits are substantially weakened if more complicated supersymmetric models are considered. RHIC energy up to $\sqrt{s} = 500$ GeV is not sufficient to produce the MSSM sparticles; however they could be within its reach if supersymmetry is realized in a more exotic scenario. Some results of "scanning" the space of squark and gluino mass parameters at RHIC are shown in Fig. 21. One can observe that, in the low mass region, the asymmetry A_L measurements at RHIC for $\tilde{q}\overline{\tilde{q}}$ and $\tilde{q}\tilde{g}$ production could be sensitive to gluino mass, although in $\tilde{q}\overline{\tilde{q}}$ process, the gluino appears only as an exchange particle. The authors of Ref. [69] conclude that, assuming the design luminosities and beam polarization of 70%, the asymmetries are statistically measurable for sparticle masses up to 75 GeV at RHIC, 350 GeV at the Tevatron and well above 1 TeV at LHC, provided experimental uncertainties on them can be kept under control.

The similar study for slepton production in polarized hadron collisions has been recently presented in Ref. [72]. However, this channel might not be accessible at RHIC, because, even in the most optimistic scenarios, the cross section is not expected to exceed 1 fb.

In the examples above, it is assumed that the polarized parton distribution functions (pol-PDFs) of initial longitudinally polarized hadrons would be known at a sufficient accuracy for being able to detect A_L deviations from the SM predictions[§]. Another venue (The best place? - J. Soffer et al. [75]) to look for a new physics beyond the SM, which does not rely this much on the precise pol-PDF knowledge, is in the observables that either vanish or are very suppressed in the SM. The good representatives of such observables are transverse spin asymmetries – single or double – for $W^{\pm}$ and Z^0 productions, since these are expected to be extremely small in the SM [73, 74, 75]. Non-vanishing contributions could arise here for example in the form of higher-twist terms, which would be suppressed as powers of $M^2/M^2_{W,Z}$, where M is a hadronic mass scale and $M_{W,Z}$ is the $W^{\pm}$ or Z^0 mass. Other possible contributions were demonstrated in Ref. [74] to be negligible as well. New physics effects, on the contrary, might generate asymmetries at leading twist.

In Ref. [75], the authors have argued that the existence of *R*-parity violating MSSM interaction would generate the single-spin azimuthal dependences[¶] of the charged lepton production via $W^{\pm}$ in collision of transversely polarized protons at unpolarized: $p^{\uparrow}p \to W^{\pm}X \to e^{\pm}\nu X$ or $\mu^{\pm}\nu X$ or $\tau^{\pm}\nu X$. The results of [75] show that, in this particular extension of the SM, the asymmetries are likely to be small and, at best, could be just marginally detectable at RHIC. Nevertheless, this does not exclude that other non-standard mechanisms produce larger effects.

One more mechanism of generating non-zero A_N and A_T asymmetries in leptoproduction

[‡] Minimal Supersymmetric Standard Model.

[§] Presumably, the pol-PDFs will be well measured as a part of the mainstream RHIC-Spin program discussed in the previous sections, as well as at the other facilities.

[¶] These are A_N and A_T asymmetries; see Refs. [75, 77] for details.

via $W^{\pm}$ and Z^0 decays is due to anomalous electroweak dipole moments of quarks [75, 76, 77]. Phenomenologically, the presence of anomalous dipole moments could be described as a combination of tensor and (pseudo)scalar $q\overline{q}W$ and $q\overline{q}Z$ couplings additional to the standard *V* and *A* couplings. The nonzero A_N and A_T arise from the interference of these additional couplings with the SM's *V* and *A* couplings. The SM predictions for anomalous dipole moments of u and d quarks, which provide the main contribution to the $W^{\pm}$ and Z^0 production at RHIC, are extremely small, and their effects are much below the RHIC sensitivity. On the other hand, the current experimental limits on anomalous dipole moments of quarks[‖] are still far above the SM expectations. The most stringent experimental constraints, applicable to *CP*-conserving components of quark dipole moments, come from the analysis [78] of electroweak data from high energy colliders. In this analysis, it has been considered that theories beyond the SM, emerging at some characteristic energy scale above W/Z mass, have effect at low energies $E \leq M_{W,Z}$, and can be introduced by taking account of an effective Lagrangian that extends the SM Lagrangian $\mathcal{L}_{SM}$: $\mathcal{L}_{eff} = \mathcal{L}_{SM} + \delta\mathcal{L}$. To preserve the consistency of the low energy theory, it has been assumed that the non-SM Lagrangian $\delta\mathcal{L}$ is $SU(3)_C \times SU(2)_L \times U(1)_Y$ gauge invariant. The $W^{\pm}$ and Z^0 productions in $p^{\uparrow}p$ collisions at RHIC is expected to have a good sensitivity on $\mathcal{L}_{SM}$–$\delta\mathcal{L}$ interference at the parton level due to strong correlations between the proton spin and polarization of high-x valence quarks, that participated in gauge boson production [79]. As it has been estimated in Ref. [77], the measurements at RHIC, carried out with transversely polarized proton in the context of the physics discussed in the previous sections, would improve the current experimental limits [78] on electroweak dipole moments of u and d quarks by a factor of ∼5–10. But a non-zero result would be a direct indication of a new physics beyond the SM.

- $W + c$ (**Yuji ?**)

- other opportunities possibly offered by high-luminosity running (and/or a new detector)
- opportunities with polarized beams in p+heavy-ion physics (**Les**)

2.10 Connection to eRHIC (Abhay)

Addition of a high energy high polarization lepton (electron/positron) beam facility to the existing RHIC Complex to be able to collide with its hadron beam would dramatically increase RHIC's capability to do precision QCD physics. Such a facility with 10 GeV/c polarized electron/positron has been proposed and is called eRHIC. There are many direct and indirect connections between the RHIC spin program and the eRHIC. We categorize them in to two groups:

- *Direct connections to RHIC Spin:* In these the physics observables measured by the existing RHIC spin physics program will be measured in complementary kinematic regions, or in some cases augmented to complete the understanding of the nucleon spin.

- *Indirect Connection to RHIC Spin:* These include measurements not possible with RHIC Spin, but are of significance to understanding QCD with spin in general or nucleon spin in particular.

[‖] And of τ-lepton.

2.10.1 Direct Connections

Directions connections between RHIC Spin and eRHIC are made on three principle topics. The measurement of polarized gluon distribution, the measurement of quark-anti-quark distributions, and on transverse physics measurements.

For polarized gluon distribution measurement eRHIC enables increase in the kinematic range and precision, particularly in the low x. At eRHIC the polarized gluon distribution will be measured using a) the scaling violations of spin structure function $g_1^{p/n}$ and b) di-jet and high pT di-hadron production in the photon gluon fusion process.[**?**] RHIC spin measurements discussed before will predominantly most significant in in the medium-high x range$x > 10^{-2}$, while eRHIC will complement them with precision on low x ($x < 10^{-2}$) all the way to $x \sim 10^{-4}$.

RHIC Spin will for the first measure model independently the polarized quark and anti-quark distributions using single longitudinal asymmetry measurements in pp scattering via ($W^{\pm}$) production. Analysis of these asymmetries would give us $\Delta u, \Delta\overline{u}, \Delta d, \Delta\overline{d}$**??**. The quark-anti-quark separation in such a way is not possible in fixed target DIS where the virtial γ is the propogator of the force which can not differentiate between quarks and anti-quarks. However at high enough energy-DIS at eRHIC, in addition virtual $W^{\pm}$ also get exchanged. If $\Delta q = u, \overline{u}, d, \overline{d}$ are known by early next decade from RHIC Spin, eRHIC will be able to continue this program in to explore the heavy quarks i.e. identify the spin contributions from $\Delta c/\overline{c}$ and $\Delta s/\overline{s}$. Of course, traditional methods to get quark flavor distributions, semi-inclusive DIS measurements using measurements of charged and neutral pions and kaons will also continue, (quark-anti-quark unseparated) would give access to low x flavor separation in parton distributions as in presently fixed target DIS experiments.

Transversity is the last as yet unmeasured spin structure function discussed in detail in **??**. The measurements at RHIC with pp scattering will be made using measurements of Collins Fragmentation Function (CFF), Interference Fragmentation Functions (IFF) and if very large luminosities are achieved, also with Drell Yan (DY) processes.[**?**] These measurements will be made in the center of mass energy range from 200 to 500 GeV. The eRHIC will make a complimentary set of measurements, with high precision using CFF and IFF measurements, not unlike those made by the HERMES collaboration presently.

Diffractive physics with polarized pp and ep: More connections?

2.10.2 Indirect Spin Connections

In addition to the measurements eRHIC will do that will extend or complement the investigation of nucleon spin with RHIC Spin, there is another class of nucleon spin and other helicity related measurements that could also be made with eRHIC. A partial list includes:

- Measurement of spin structure functions g_1 of the proton and neutron and the difference between then that tests the Bjorken spin sum rule. eRHIC will do this with accuracies that will for the first time start competing and challenging the experimental systematic uncertainties at the level of 1- 2%. Low x phenomenon has been one of the most exciting aspect

of the physics that developed in the unpolarized DIS measurements in the last decade, and eRHIC will probe that low x kinematics for the first time with polarized beams

- eRHIC will be the only possible facility in the foreseeable future at which QCD spin structure of the virtual photon could be explored. The process employed for this investigation is that of photon gluon fusion[**?**].

- Deeply virtual compton scattering (DVCS) for final state photons as well as other vector mesons measured using al most complete acceptance (4π) detectors has been suggested as a preliminary requirement toward the measurement of the Generalized Parton Distributions (GPDs). A series of different GPD measurements may be required eventually to extract the orbital angular momentum of the partons. This is the last part of the nucleon spin puzzle which we may have to address after the spin of the gluon is understood. Although the theoretical formulation is not yet ready, it is expected that by the time the eRHIC comes on line, there will be a formalism available to take the measured GPDs and determine the orbital angular momentum of partons. These measurements at eRHIC will be complementary, at much higher energy scales, to those being planned at Jefferson Laboratory with its 12 GeV upgrade plan.

- Drell Hern Gerasimov spin rule measurements presently underway at Jefferson laboratory[**?**] and at MAMI [**?**] are mostly at low value of ν[**?**]. While the significance of the contribution the spin sum rule from high ν is small, absolutely no measurements exist beyond the value of $\nu >\approx 1$ GeV. eRHIC will extend direct measurements of the high ν components to up to 500 GeV.

- Precesions measurements of spin structure functions in very high x ~ 0.9 region could be part of the eRHIC physics program with specially designed detectors as has been discussed in [**?**].

In summary, while the physics programs with polarized proton beams at RHIC and eRHIC have much in the way of complementarity of physics measurements, the way to success at eRHIC passes through a successful RHIC spin program not only at 200 GeV in center of mass but also at 500 GeV in center of mass.

3 Accelerator performance (Mei & Wolfram)

Polarized proton beams were accelerated, stored and collided in RHIC at a proton energy of 100 GeV. The average store luminosity reached $4 \times 10^{30}\mathrm{cm}^{-2}\mathrm{s}^{-1}$, and the average store polarization 40% (see Tab. 3). Over the next 4 years we aim to reach the Enhanced Luminosity goal for polarized protons, consisting of an average store luminosity of

- **$60\times10^{30}\mathbf{cm}^{-2}\mathbf{s}^{-1}$ for 100 GeV** proton energy, and
- **$150\times10^{30}\mathbf{cm}^{-2}\mathbf{s}^{-1}$ for 250 GeV** proton energy,

both with an **average store polarization of 70%**. Tab. 3 gives a projection of the luminosity and polarization evolution through FY2008. Luminosity numbers are given for 100 GeV proton energy and one interaction point, with collisions at two interaction points. For operation with

more than two experiments, the luminosity per interaction point is reduced due to an increased beam-beam interaction. For each year the maximum achievable luminosity and polarization is projected. Projections over several years are not very reliable and should only be seen as guidance for the average annual machine improvements needed to reach the goal. We do not give a minimum projection as we usually do in Ref. [80], since the minimum projection is based on proven performance, and no long polarized proton run was done so far. We also assume that 10 weeks of physics running are scheduled every year to allow for commissioning of the improvements and development of the machine performance.

Table 3: Maximum projected RHIC polarized proton luminosities through FY2008. Luminosity numbers are given for 100 GeV proton energy and one interaction point, with collisions at two interaction points. 10 weeks of physics operation per year are assumed.

Fiscal year		2002A	2003A	2004A	2005E	2006E	2007E	2008E
No of bunches	...	55	55	56	79	79	100	112
Protons/bunch, initial	10^{11}	0.7	0.7	0.7	1.0	1.4	2.0	2.0
β^*	m	3	1	1	1	1	1	1
Peak luminosity	$10^{30}\mathrm{cm}^{-2}\mathrm{s}^{-1}$	2	6	6	16	31	80	89
Average luminosity	$10^{30}\mathrm{cm}^{-2}\mathrm{s}^{-1}$	1.5	3	4	9	21	53	60
Time in store	%	30	41	41	50	53	56	60
Max luminosity/week	pb^{-1}	0.2	0.6	0.9	2.8	6.6	18.0	21.6
Max integrated luminosity	pb^{-1}	0.5	1.6	3	20	46	126	151
Average store polarization	%	15	30	40	45	65	70	70
Max LP^4/week	nb^{-1}	0.1	5	23	120	1180	4330	5190

In Fig. 22 the integrated luminosity delivered to one experiment is shown through FY2012 for two scenarios: 10 weeks of physics operation per year, and 10 weeks of physics operation every other year. The integrated luminosities differ by about a factor of 3. For every projected year shown in Fig. 22 the weekly luminosity starts at 25% of the final value, and increases linearly in time to the final value in 8 weeks. During the remaining weeks the weekly luminosity is assumed to be constant at the values listed in the table. For the scenario with 10 weeks of physics operation every other year, the final values are not increased in years without proton operation, since no time is available to develop the machine performance. Thus in our projections we reach the Enhanced Luminosity goal in FY2008 with 10 week physics operation per year, but need until FY2011 with 10 weeks of physics operation every other year.

For operation at 250 GeV proton energy, the luminosity projections need to be multiplied by 2.5. We expect no significant reduction in the averages store polarization after full commissioning of polarized proton ramps to 250 GeV.

3.1 Polarization limitations

The RHIC beam polarization at 100 GeV is currently limited by the AGS beam polarization transmission efficiency of about 70%, and the source polarization. With the installation of a new solenoid in FY2005, the source polarization is expected to increase from 80% to 85%. The existing AGS polarized proton setup includes a 5% warm helical snake for overcoming imperfection spin depolarizing resonances and an RF dipole for overcoming 4 strong intrinsic spin resonances. This setup has two drawbacks:

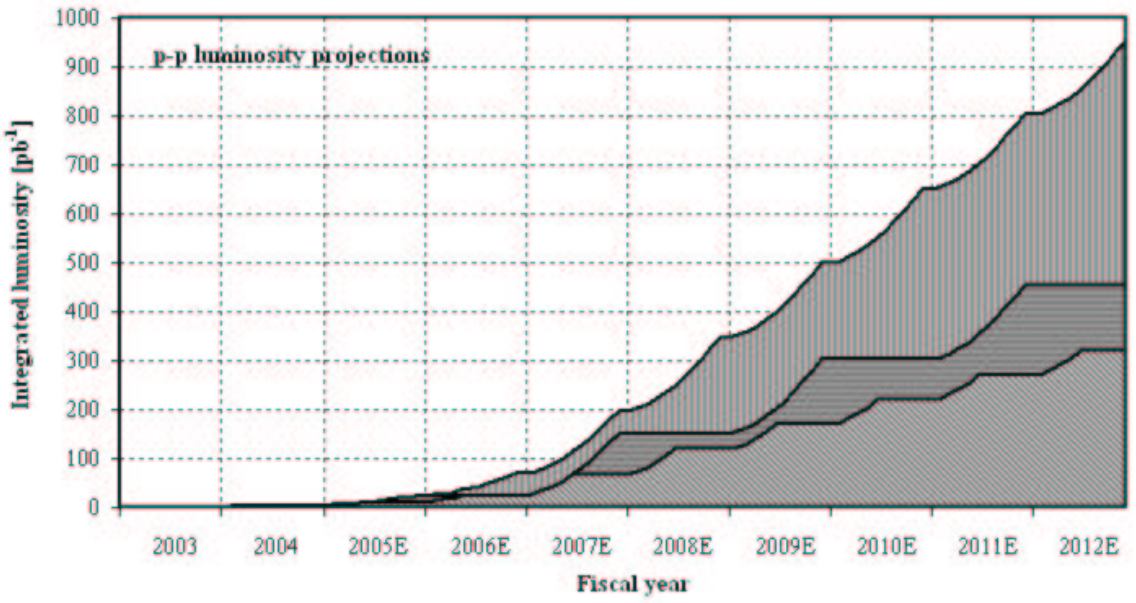

Figure 22: Maximum projected integrated luminosity through FY2012 for 10 weeks of physics operation per year, and 10 weeks of physics operation every other year. Luminosity numbers are given for 100 GeV proton energy and one interaction point, with collisions at two interaction points.

1. All the weak intrinsic spin resonances are crossed with no correction and result in a total depolarization of about 16%.
2. Operation with the RF dipole still leads to about 15% depolarization.

In addition, the AGS has shown a dependence of the beam polarization on the bunch intensity. These shortcomings can be overcome with the installation of a new AGS cold snake, to be initially commissioned in 2005. With a scheme that combines the AGS cold snake of 15%, and the AGS warm snake of 5%, depolarizations at all imperfection and all intrinsic spin resonances should be eliminated, making the AGS spin transparent with the exception of some mismatch at injection and extraction.

Obtaining 70% beam polarization in RHIC at 250 GeV is challenging because of strong intrinsic and imperfection resonances beyond 100 GeV. Betatron tunes and orbit distortions have to be controlled precisely to avoid depolarization due to snake resonances. Simulations show that orbit distortions have to be corrected to less than 0.3 mm rms. Orbit errors are introduced due to misalignments and remain if the orbit cannot be corrected completely. A realignment of the entire ring is scheduled for the 2005 summer shutdown. Efforts continue to improve the existing beam position monitor system, and the orbit correction techniques. A beam-based alignment technique is under development. With the existing hardware and software, orbit distortions of 1 mm rms were achieved, as measured by the beam position monitors. Acceleration of polarized proton beams beyond 100 GeV is planned in 2005. The result of this machine development effort will provide guidance for the tolerable levels of machine misalignments and orbit errors.

3.2 Luminosity limitations

A number of effects limit the achievable luminosity. Currently the bunch intensity is limited to about 1×10^{11} to maintain maximum polarization in the AGS. This restriction should be removed with the AGS cold snake. With intense bunches the beam-beam interaction will limit the luminosity lifetime. With bunches of 2×10^{11} protons and 2 interaction points, the total beam-beam induced tune spread will reach 0.015. Operation with more than two collision will significantly reduce the luminosity lifetime. High intensity beams also lead to a vacuum breakdown, caused by electron clouds. In the warm sections, NEG coated beam pipes are installed, that have a lower secondary electron yield, and provide linear pumping. In the cold regions, additional pumps are installed to improve the vacuum to an average value of 10^{-5} Torr before the cool-down starts. With the PHENIX and STAR detector upgrades, the vacuum system in the experimental regions will also be improved.

Time in store can be gained through faster machine set-up, a reduction in system failures, and the injection of multiple bunches in each AGS cycle. We project that the time in store can be increased to about 100 hours per week, or 60% of calendar time.

3.3 Polarimetry

Beam polarization measurements in RHIC provide immediate information for performance monitoring, and absolute polarization to normalize the experimental asymmetry results. Two types of polarimeters are used. Both are based on small angle elastic scattering, where the sensitivity to the proton beam polarization comes from the interference between the electromagnetic spin-flip amplitude that generates the proton anomalous magnetic moment and the hadronic spin non-flip amplitude, and possibly a hadronic spin-flip term.

One type of polarimeter uses a micro-ribbon carbon target, and provides fast relative polarization measurements. The other type uses a polarized atomic hydrogen gas target, and provides slow absolute polarization measurements. In addition, both PHENIX and STAR have developed local polarimeters that measure the residual transverse polarization at their interaction points. These polarimeters are used to tune and monitor the spin rotators that provide longitudinal polarization for the experiments. They polarimeters are discussed in the Experiments section.

The fast proton-carbon polarimeter was first developed at the IUCF and the AGS [81]. It measures the polarization in RHIC to $\Delta P = \pm 0.02$ in 30 seconds. Measurements taken during a typical store in 2004 are shown in Fig. 23. A carbon ribbon target is introduced into the beam, and the left-right scattering asymmetry of recoil carbon ions is observed with silicon detectors inside the vacuum. The silicon detectors observe the energy and time of flight of the recoil particles near 90° [82]. The detector selects carbon ions with a momentum transfer in the coulomb-nuclear interference (CNI) region, $-t = 0.005 - 0.02$ (GeV/c)^2. In this region, the interference of the electromagnetic spin flip amplitude and the hadronic non-flip amplitude produces a calculable t-dependent asymmetry of 0.03 to 0.02. The cross section is large, so that the sensitivity to polarization is large. A term from a hadronic spin flip amplitude is also possible and is reported in Ref. [81]. This contribution is not calculable, so that this polarimeter must be calibrated using a beam of a known polarization.

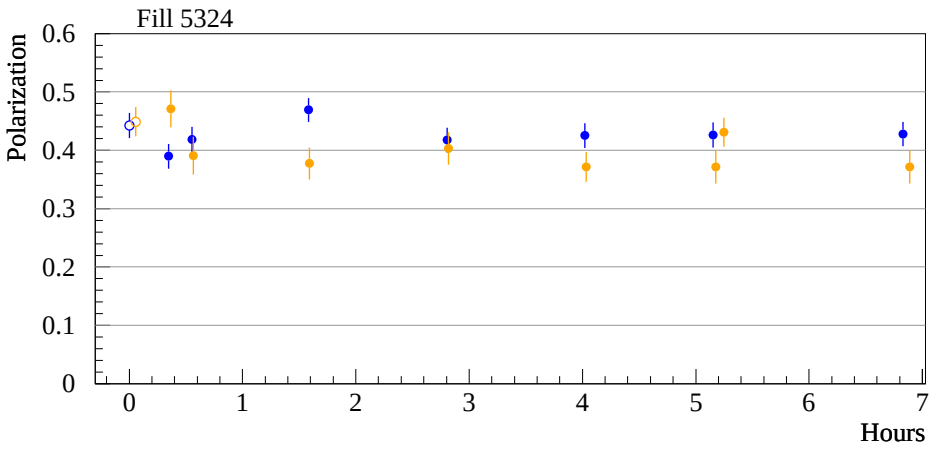

Figure 23: Measured polarization during one store of RHIC in 2004.

A polarized atomic hydrogen gas jet target was used for the first time in RHIC in 2004 [83]. The atoms are polarized with the Stern-Gehrlach process to give electronic polarization, with rf transition to select proton polarization. The atoms are focused in the RHIC beam region to 6 mm FWHM using the atomic hydrogen magnetic moment. A Breit-Rabi polarimeter after the RHIC beam measures the polarization by cycling through rf transition states. The polarization was determined to be 0.92 ± 0.02, including correction for the measured 2% molecular fraction (4% nuclear fraction) that is unpolarized. Silicon detectors observe a left-right asymmetry for proton-proton elastic scattering in the CNI region, similar to the p-carbon polarimeters. By measuring the asymmetry with respect to the target polarization sign, flipped every 8 minutes in 2004 by changing rf transitions, we measure the analyzing power for proton-proton elastic scattering. This is shown in Fig. 24. This (preliminary) result from 2004 provides the most sensitive measurement of A_N, as can be seen in the figure. By then measuring the left-right asymmetry with respect to the beam polarization sign, flipping each bunch (every 200 ns), we obtain the absolute beam polarization. The absolute beam polarization was measured to about $\Delta P/P = 7\%$ in 2004 (preliminary).

A remaining issue is whether the carbon polarimeter calibration can be used for different detectors, from year to year, or whether it will be necessary to recalibrate each year using the jet target. We can also choose to use the jet target as the RHIC polarimeter, with the carbon polarimeter used for corrections, for example for different polarization of the bunches and for a polarization profile of the beams.

3.4 Long-term perspective

A number of ideas are pursued for long-term improvements of the machine performance. RHIC II aims at increasing the heavy ion luminosity by an order of magnitude through electron cooling. For protons, cooling at store is not practical but pre-cooling at injection might be beneficial. A further reduction of β^*, especially at 250 GeV proton energy appears possible. Some benefits may also come from stochastic cooling, currently developed for heavy ions. We expect a luminosity improvement of a factor 2-5 for polarized protons for RHIC II.

With a new interaction region design, the final focusing quadrupoles can be moved closer

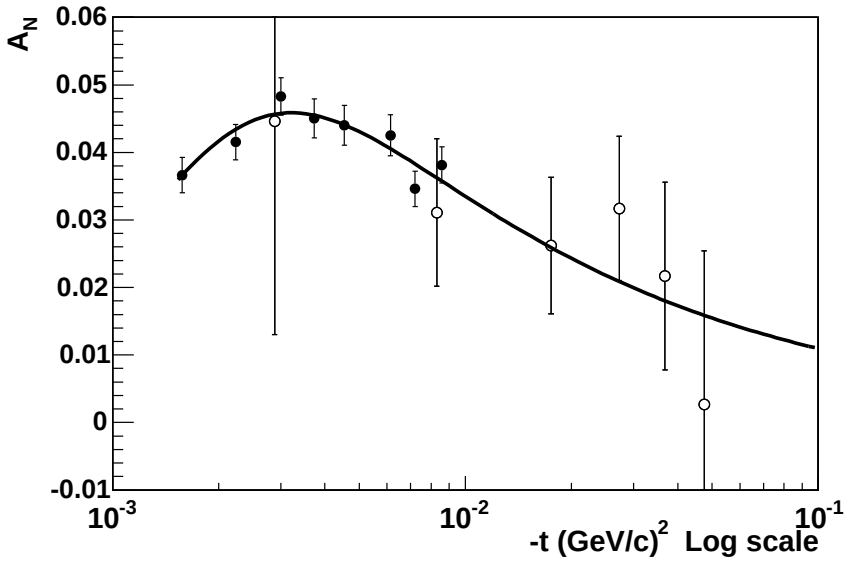

Figure 24: A_N for proton-proton elastic scattering in the CNI region, measured using the polarized atomic hydrogen jet target in RHIC [83]. The open circles are data from E704 at Fermilab [84].

to the interaction point, thus allowing to squeeze β^* further. This, however, makes some space unavailable for the detectors. Additional increases in the luminosity may come from a further increase in the number of bunches, to close to 360, as is planned for eRHIC, or operation with very long bunches. The latter requires a substantial R&D effort, as well as a new timing system for the detectors.

4 Experiments

4.1 Phenix (Matthias)

- present status & issues to solve
- priorities
- planned upgrades and developments
- required resources

4.2 Star (Steve)

RHIC Spin Report for DOE: Outline of STAR Detector Section 4.2 (each major heading represents 1 paragraph)

A. Overview of STAR detector and collaboration

1. Figure: cross section of STAR, emphasizing subsystems already added with spin program

as primary driver. 2. Brief description of BBC's and FPD's and their use for spin program: Figure of BBC asymmetries vs. CNI asymmetries, with STAR rotators on and off. 3. Status of barrel and endcap EMCs; timeline to complete BEMC readout. 4. Use of EMCs in p+p triggers for jets, photons, (0, W, J/(. 5. Recent expansions of collaboration interests in spin program.

B. Performance of STAR EMC's

1. Figure: photo of insertion of last BEMC module; photo of completed EEMC. 2. Figure: event display of dijet with TPC and BEMC; jet neutral/total ET spectrum from BEMC + TPC in 2004 p+p run. 3. Figure: typical SMD profile and (0 invariant mass spectrum from EEMC for 2004 p+p run. 4. Brief description of ongoing algorithm development for (0 and (ID.

C. Motivation for STAR upgrade needs for spin program

1. Improved forward tracking: TPC resolution limits at 40 GeV/c, especially in endcap region; need for W charge sign discrimination, improved e/h discrimination for W program; fast tracking minimizes TPC pileup ambiguities. 2. Figure: charge sign discrimination improvements with model forward tracking vs. TPC alone. 3. Forward extension of calorimetry: primary motivation from studying low-x gluons in nuclei; benefits to spin program in low-x and large ((access. 4. Benefits to spin from planned STAR upgrades driven by other physics: TOF pion ID for interference fragmentation studies of transversity (?); DAQ upgrades, rate capability, space-saving for forward tracker; Heavy Flavor Tracker for improved ID of open charm, beauty, sensitivity to quark mass terms in QCD, etc.

D. Plan for forward tracking improvements

1. Figure: schematic illustrations of inner silicon barrels and disks, and of endcap GEM tracker under consideration. 2. Envisioned timeline (rough), staging and integration with other STAR upgrades. 3. Organization of efforts and institutions involved; R&D activities under way. 4. Rough estimate of resources needed to design/construct. 5. Open issues to address: optimum tradeoffs between coverage and cost; resolution impact of material at endcap of TPC; others?

E. Plan for Forward Meson Spectrometer

1. Figure: transverse profile of proposed calorimeter, and location within STAR. 2. Institutions involved, cost estimate, source of materials and funding, MRI proposal submitted to NSF. 3. Timeline driven by d+Au gluon saturation studies. 4. Open issues to address?

4.3 Other experiments

- Brahms (**Flemming**)
- New detector
- eRHIC detector

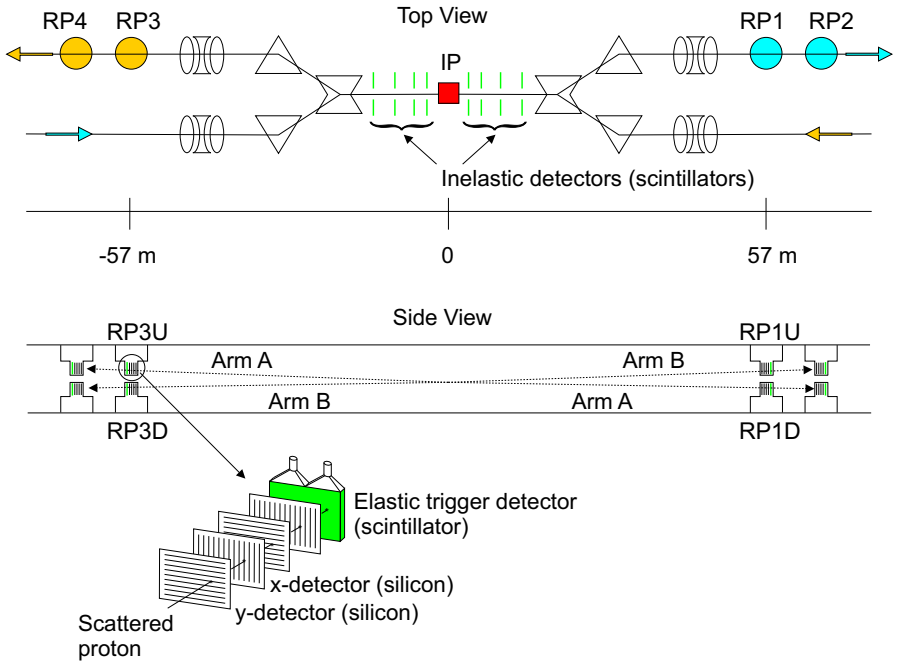

Figure 25: Layout of the pp2pp experiment. Note the detector pairs RP1, RP2 and RP3, RP4 lie in different RHIC rings. Scattering is detected in either one of two arms: Arm A is formed from RP3U and RP1D. Conversely, Arm B is formed from RP3D and RP1U.

4.3.1 PP2PP running with the current setup (Wlodek)

With a small modification requiring rotation of RP2 and RP4 to horizontal orientation, the present experimental setup, see Fig. **??** is suitable for additional measurements in an extended $|t|$-range. At $\sqrt{S}$ = 200 GeV one can use the capacity of existing power supplies to run with the accelerator optics of β^* = 20 m. The β^* = 20 m tune at $\sqrt{S}$ = 200 GeV makes it possible to extend the kinematic coverage to a lower $|t|$ of $0.003 < |t| < 0.020$ (GeV/c)^2. At $\sqrt{S}$ = 500 GeV the optics with β^* = 10 m will be used, allowing measurements up to $|t| \approx 0.12$ (GeV/c)^2.

The result obtained in Run 2003 is shown in Fig. **??**. With the modification of the setup described above one will be able to improve the A_N measurements, measure $A_N N$. This will certainly help resovle the isue of the presence of the hadronic spin flip amplitude at high energies.

With six million elastic events, a statistical error of $\Delta\epsilon_N$ = 0.0017 for each of six points of the raw counting rate asymmetry in the interval $0.003 < |t| < 0.020$ (GeV/c)^2 can be obtained. The analyzing power is related to the raw asymmetry by $A_N = \frac{\epsilon_N}{P_{yellow}+P_{blue}}$. Assuming a beam polarization of $P_{yellow} = P_{blue} = 0.4 \pm 0.1$ for each of the two beams would lead to a statistical error of ΔA_N = 0.004 for each of the six data points. The data taking time, extrapolated from the running conditions obtained in run 2 and considering the changed β^*, for six million elastic events would be about 20 hours.

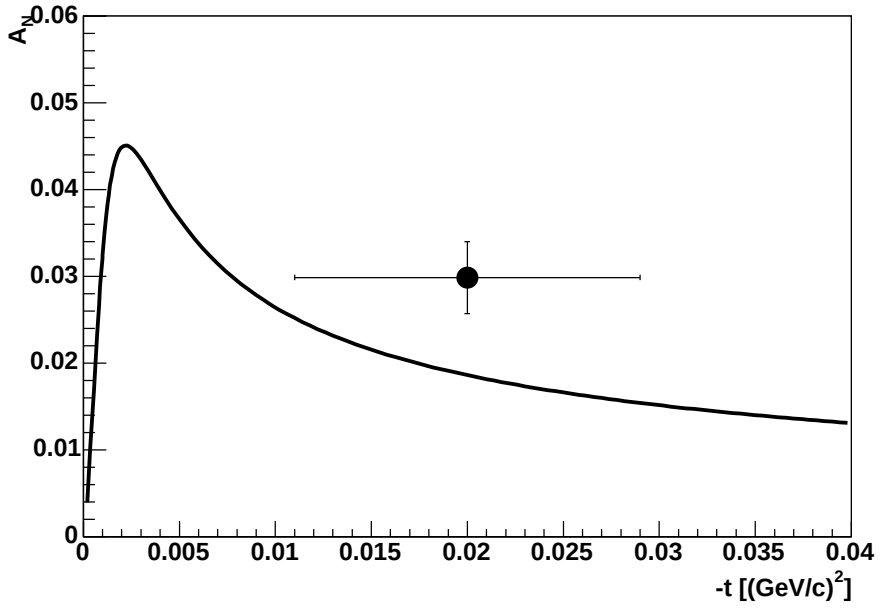

Figure 26: The single spin analyzing power A_N for the full interval. Vertical error bars show statistical errors, horizontal error bars show the $|t|$-range. Solid curve corresponds to theoretical calculations without hadronic spin flip[**?**].

The measurement of the double-spin asymmetry, A_{NN}, depends on the measurement of the relative luminosities, needed for normalization of the four spin-dependent counting rates involved. In addition, the statistical error depends on the square of the beam polarization. With the above assumptions for beam polarization and error, a value of 0.01 for A_{NN}, and six million elastically scattered protons, the error on the double-spin asymmetry was estimated to be $\Delta A_{NN} = 0.03$ for a single data point over the entire $|t|$-range. A high beam polarization and small error on the polarization measurement are very important.

- jet (**Sandro**)

5 Spin plan schedule (Gerry)

In the charge, we were requested to consider two running schedules: 10 and 5 physics weeks on spin per year. These follow, showing *example* plans. We emphasize that we expect that the actual run plan will be developed from the experiment beam use proposals. Our consideration of these scenarios should not suggest that we advocate a change to this successful approach.

A key issue is the completion of experiment hardware to run the W physics program. The required hardware are the muon trigger improvements for PHENIX, and a forward tracker for STAR. The PHENIX improvements are being proposed to NSF ($1.8M for resistive plate chambers) and to the Japan Society for Physical Sciences ($1.0M for muon tracking readout electronics), with a planned completion for the 2008 RHIC run. The STAR tracker is planned to be

proposed to DOE (estimated $5M) in 2006, and to be complete for the 2010 run.

The example plan below for the 10 physics week/year case is "technically driven". The plan assumes that the funding is received, and the work is completed as planned. For the 5 week plan, the delay in reaching luminosity goals for $\sqrt{s}$=200 GeV delays the start of the W running considerably, by greater than three years. An early completion of the W hardware is less of an issue for this case.

A second key issue is machine performance. We assume that we reach the polarization goal of 70% in 2006. For luminosity, we assume in the example plan that we reach two thirds of the "maximum" luminosity (see section 3). This assumption is discussed there.

A third key issue is experiment availability, in which we include up time, live time, and the fraction of the collision vertex accepted by the experiment. This results in "recorded luminosity" for each experiment. We have taken the up time to be 70% for each experiment, as has been achieved. The live time for PHENIX is 90%, due to multi-event buffering; the live time for STAR is 50%. The online data selection adjusts thresholds, for example the lower p_T requirement, to reach these live time levels. The PHENIX vertex acceptance for the 200 GeV running is 60%, requiring the vertex to be within 20 cm of the IP. We have used this acceptance also for 500 GeV. The STAR vertex acceptance contains all collisions. The overall factor for recorded/delivered luminosity for both experiments is 35%. The physics sensitivities shown in section 2 also include apparatus acceptance and event selection acceptance.

5.1 10 physics weeks

Table 5 shows the example spin plan for 10 physics weeks per year, with a *technically driven* schedule. The 200 GeV running continues through 2008, with a total of 300 pb^{-1} delivered, and 100 pb^{-1} recorded luminosity by both PHENIX and STAR. By the year 2009, the PHENIX muon triggering improvements are complete, and the STAR forward tracking is partially in place, and complete for the 2010 run. The year 2009 is considered an engineering run, for both the accelerator and the experiments. By the completion of the year 2012, for 500 GeV, 800 pb^{-1} luminosity is delivered, and 300 pb^{-1} recorded by each experiment. These luminosities and polarizations provide the physics sensitivities presented in section 2.

5.2 5 physics weeks

Table **??** gives the example spin plan for 5 physics weeks per year, which we have interpreted to mean 10 physics weeks each two years to reduce the end effects. As has been presented in section 3, the delay in the RHIC spin physics results is actually greater than a factor of two, compared to 10 physics weeks each year. This is due to an assumed "turn-on" period of reaching the instantaneous luminosity maximum that is based on our experience, from the heavy ion program. In any case, the programs are stretched out to over 6 years for the gluon polarization measurements at 200 GeV, and an additional 6 years or more for the W physics program. The proposed measurements would be completed in 2018 or later.

Table 4: RHIC spin example schedule, 10 physics weeks per year, technically driven.

Fiscal year	Spin Weeks	CME(GeV)	P	L(pb^{-1}	Remarks
2002	8	200	0.15		First pol. pp collisions! Transverse spin
2003	10	200	0.27		Spin rotators commissioned, first helicity measurements
2004	1	200	0.4		New betatron tune developed, first jet absolute meas. P
2005	9	200	0.5	10-20	$A_{LL}(\pi^0, jet)$, also 500 GeV studies
2006	10	200	0.7		AGS Cold Snake commissioned, NEG vacuum coating complete
2007	0				
2008	20	200	0.7		Direct γ, completes goal for 200 GeV running
2009	10	500	0.7		PHENIX muon arm trigger installed, eng. run
2010	10	500	0.7		STAR forward tracker installed, W physics
2011	10	500	0.7		
2012	10	500	0.7		Completes 500 GeV goal

Table 5.2 RHIC spin example schedule, 5 physics weeks per year.

6 Summary (Gerry)

In this document we have described the RHIC spin research plan, responding to the request by the Department of Energy Office of Nuclear Physics. We were requested to cover 1) the science, 2) the requirements for the accelerator, 3) the resources that are needed and timelines, and 4) the impact of a constant effort budget to the program.

1) The science is presented in section 2. Here we have emphasized measuring gluon polarization and anti-quark polarization in the proton. RHIC will provide the first sensitive measurements of each. We believe this is an exciting program, which addresses the structure of matter.

2) The accelerator requirements are presented in section 3. We are well along in reaching the polarization requirement of 70%, and anticipate reaching this goal in 2006, for 200 GeV running. To reach this goal for 500 GeV running will require releveling the machine, which is planned. Reaching the luminosity goal will be challenging. We must store 2×10^{11} polarized protons in 110 rf bunches in each RHIC ring and collide them. Limits of betatron tune shift and of electron cloud formation will be tested. For the physics sensitivities presented, we have used a luminosity of 2/3 of the calculated maximum.

Table 5: RHIC spin example schedule, 10 physics weeks per year.

Fiscal year	Spin Weeks	CME(GeV)	P	L(pb^{-1}	Remarks
2005	9	200	0.5	10-20	$A_{LL}(\pi^0, jet)$, also 500 GeV studies
2006-2007	10	200	0.7		AGS Cold Snake commissioned, NEG vacuum coating complete
2008-2009	10	200	0.7		Direct γ
2010-11	10	200	0.7		completes goal for 200 GeV running
20012-13	10	500	0.7		PHENIX muon arm trigger installed, eng. run
2014-2015	10	500	0.7		STAR forward tracker installed, W physics
2016-2017	10	500	0.7		
2018-2019	10	500	0.7		Completes 500 GeV goal

3) The required experiment resources are presented in section 4. The PHENIX and STAR detectors are complete for the gluon polarization program. Both need improvements to be ready for the W physics program. These are described in the section. For a "technically driven" program, where the improvements are funded and completed as proposed, the PHENIX detector will be ready for W physics in 2009, and the STAR detector in 2010.

There are also important planned upgrades for the heavy ion and spin programs that greatly extend the range of spin physics, and these are also described in section 4.

4) The impact of a constant effort budget is presented in section 5, where we compare the two plans, as requested in the charge to the RHIC Spinplan Group:

"I ask that you consider two RHIC Spin running scenarios: 1) 5 spin physics data taking weeks per year (averaged over two years using the combined fiscal year concept); 2) 10 spin physics data taking weeks per year. These two scenarios will give appropriate indications of the physic goals that can be met over a period of years without involving the Group in difficult funding and cost scenarios that are not central to the calculation of physics accomplishments over time." (Appendix A)

The plan with 10 spin physics weeks per year, the technically driven plan, completes the gluon polarization measurements and the W physics measurements by 2012.

The plan with 5 spin physics weeks per year completes this program in 2019 or later. With this plan RHIC runs 25% of the year on average (we assume 10 spin physics weeks per two year cycle).

Acknowledgments

References

[1] J.C. Collins, D. Soper and G. Sterman, in A.H. Mueller, ed., *Perturbative Quantum Chromodynamics* (World Scientific 1989), hep-ph/0409313.

[2] S. Kretzer, Phys. Rev. **D62** 054001 (2000); B. Kniehl, G. Kramer and B. Pötter, Nucl. Phys. **B582** 514 (2000); Nucl. Phys. **B597** 337 (2001); L. Bourhis, M. Fontannaz, J.P. Guillet, M. Werlen, Eur. Phys. J. **C19** 89 (2001); S. Kretzer, E. Leader, E. Christova, Eur. Phys. J. **C22**, 269 (2001).

[3] C. Bourrely and J. Soffer, hep-ph/0311110.

[4] PHENIX Collaboration (S.S. Adler et al.), Phys. Rev. Lett. **91**, 241803 (2003); STAR Collaboration (J. Adams et al.), Phys. Rev. Lett. **92**, 171801 (2004).

[5] B. Jäger, A. Schäfer, M. Stratmann and W. Vogelsang, Phys. Rev. **D67**, 054005 (2003).

[6] OPAL Collaboration (G. Abbiendi et al.), Eur. Phys. J. **C37**, 25 (2004).

[7] B. E. Bonner *et al.*, Phys. Rev. Lett. **61**, 1918 (1988); A. Bravar *et al.*, *ibid.* **77**, 2626 (1996); D. L. Adams *et al.*, Phys. Lett. B **261**, 201 (1991); **264**, 462 (1991); Z. Phys. C **56**, 181 (1992).

[8] G. L. Kane, J. Pumplin, and W. Repko, Phys. Rev. Lett. **41** 1689 (1978).

[9] K. Krueger *et al.*, Phys. Lett. B **459**, 412 (1999); C. E. Allgower *et al.*, Phys. Rev. D **65**, 092008 (2002).

[10] A. Airapetian *et al.*, Phys. Rev. Lett. **84**, 4047 (2000); Phys. Lett. B **535**, 85 (2002); **562**, 182 (2003).

[11] A. Bravar *et al.*, Nucl. Phys. Proc. Suppl. **79**, 520 (1999).

[12] J. Adams*et al.*, Phys. Rev. Lett. **92** (2004) 171801; A. Ogawa, 16th International spin physics symposium (SPIN2004) proceedings hep-ex/0412035.

[13] D. W. Sivers, Phys. Rev. **D41** 83 (1990)

[14] J. C. Collins, Nucl. Phys. **B396** 161 (1993); J. C. Collins, S. F. Heppelmann, G. A. Ladinsky, Nucl. Phys. **B396** 161 (1993);

[15] D. Boer, AIP Conf. Proc. **675** 479-483 (2003).

[16] J. Qiu and G. Sterman, Phys. Rev. D59, 014004 (1999).

[17] Y. Koike, AIP Conf. Proc. **675**, 449 (2003).

[18] M. Anselmino, M. Boglione, and F. Murgia, Phys. Rev. D **60**, 054027 (1999); M. Boglione and E. Leader, Phys. Rev. D **61**, 114001 (2000).

[19] M. Anselmino, M. Boglione, and F. Murgia, Phys. Lett. B **362**, 164 (1995); M. Anselmino and F. Murgia, *ibid.* **442**, 470 (1998); U. D'Alesio and F. Murgia, AIP Conf. Proc. **675** 469 (2003).

[20] M. Anselmino *et. al.* **hep-ph/0408356**; U. D'Alesio, Proceedings of Spin2004

[21] M. Boglione, E. Leader, Phys. Rev. **D61** 114001 (2000).

[22] J. Soffer, Phys. Rev. Lett. **74** 1292 (1995).

[23] D. Boer, W. Vogelsang, Phys. Rev. **D69** 094025 (2004).

[24] B. Jaffe *et al.*, Phys. Rev. bf D57 5920 (1998); J. Tang, hep-ph/9807560 and J. Tang, Thesis, MIT (1999).

[25] X. Artru, J. Collins, Z. Phys. **C69** 277 (1996); D. Boer, R. Jakob, P. J. Mulders, Phys. Lett. **B424** 143 (1998).

[26] M. Grosse Perdekamp, A. Ogawa, K. Hasuko, S. Lange, V. Siegle, Nucl. Phys. **A711** 69 (2002).

[27] A. Mukherjee, M. Stratmann and W. Vogelsang, Phys. Rev. **D67** 114006 (2003).

[28] M. Anselmino, U. D'Alesio, F. Murgia, Phys. Rev. **D67** 074010 (2003).

[29] M. Anselmino, V. Barone, A. Drago, N. N. Nikolaev, Phys. Lett. **B594** 97 (2004).

[30] M. Anselmino, M. Boglione, U. D'Alesio, E. Leader, F. Murgia, Phys. Rev. **D70** 074025 (2004)

M. Anselmino, V. Barone, A. Drago, N. N. Nikolaev, Phys. Lett. **B594** 97 (2004).

[31] G. L. Kane, J. Pumplin, and W. Repko, Phys. Rev. Lett. **41**, 1689 (1978).

[32] B. E. Bonner *et al.*, Phys. Rev. Lett. **61**, 1918 (1988); A. Bravar *et al.*, *ibid.* **77**, 2626 (1996); D. L. Adams *et al.*, Phys. Lett. B **261**, 201 (1991); **264**, 462 (1991); Z. Phys. C **56**, 181 (1992).

[33] K. Krueger *et al.*, Phys. Lett. B **459**, 412 (1999); C. E. Allgower *et al.*, Phys. Rev. D **65**, 092008 (2002).

[34] A. Airapetian *et al.*, Phys. Rev. Lett. **84**, 4047 (2000); Phys. Lett. B **535**, 85 (2002); **562**, 182 (2003).

[35] A. Bravar *et al.*, Nucl. Phys. Proc. Suppl. **79**, 520 (1999).

[36] J. Adams*et al.*, Phys. Rev. Lett. **92** (2004) 171801; A. Ogawa, 16th International spin physics symposium (SPIN2004) proceedings hep-ex/0412035.

[37] D. W. Sivers, Phys. Rev. **D41** 83 (1990)

[38] J. C. Collins, Nucl. Phys. **B396** 161 (1993); J. C. Collins, S. F. Heppelmann, G. A. Ladinsky, Nucl. Phys. **B396** 161 (1993);

[39] D. Boer, AIP Conf. Proc. **675** 479-483 (2003).

[40] J. Qiu and G. Sterman, Phys. Rev. D59, 014004 (1999).

[41] Y. Koike, AIP Conf. Proc. **675**, 449 (2003).

[42] M. Anselmino, M. Boglione, and F. Murgia, Phys. Rev. D **60**, 054027 (1999); M. Boglione and E. Leader, Phys. Rev. D **61**, 114001 (2000).

[43] M. Anselmino, M. Boglione, and F. Murgia, Phys. Lett. B **362**, 164 (1995); M. Anselmino and F. Murgia, *ibid.* **442**, 470 (1998); U. D'Alesio and F. Murgia, AIP Conf. Proc. **675** 469 (2003).

[44] M. Anselmino *et. al.* **hep-ph/0408356**; U. D'Alesio, Proceedings of Spin2004

[45] M. Boglione, E. Leader, Phys. Rev. **D61** 114001 (2000).

[46] J. Soffer, Phys. Rev. Lett. **74** 1292 (1995).

[47] D. Boer, W. Vogelsang, Phys. Rev. **D69** 094025 (2004).

[48] B. Jaffe *et al.*, Phys. Rev. bf D57 5920 (1998); J. Tang, hep-ph/9807560 and J. Tang, Thesis, MIT (1999).

[49] X. Artru, J. Collins, Z. Phys. **C69** 277 (1996); D. Boer, R. Jakob, P. J. Mulders, Phys. Lett. **B424** 143 (1998).

[50] M. Grosse Perdekamp, A. Ogawa, K. Hasuko, S. Lange, V. Siegle, Nucl. Phys. **A711** 69 (2002).

[51] A. Mukherjee, M. Stratmann and W. Vogelsang, Phys. Rev. **D67** 114006 (2003).

[52] M. Anselmino, U. D'Alesio, F. Murgia, Phys. Rev. **D67** 074010 (2003).

[53] M. Anselmino, V. Barone, A. Drago, N. N. Nikolaev, Phys. Lett. **B594** 97 (2004).

[54] M. Anselmino, M. Boglione, U. D'Alesio, E. Leader, F. Murgia, Phys. Rev. **D70** 074025 (2004)

M. Anselmino, V. Barone, A. Drago, N. N. Nikolaev, Phys. Lett. **B594** 97 (2004).

[55] F. Paige and M. J. Tannenbaum, cited in R. Ruckl, *J. de Phys.* **46**, C2-55 (1985) and T. L. Trueman, *ibid.*, C2-721.

[56] E. J. Eichten, K. D. Lane and M. E. Peskin, *Phys. Rev. Lett.* **50**, 811 (1983).

[57] CDF Collaboration, F. Abe, *et al., Phys. Rev. Lett.* **68**, 1104 (1992); *ibid.* **77**, 438 (1996). See also New York Times, Feb 8, 1996.

[58] J.-M. Virey, in *Beyond the Desert 1997, Proceedings of 1st International Conference on Particle Physics Beyond the Standard Model*, 8-14 Jun 1997, Castle Ringberg, Germany, hep-ph/9707470. See also, J. Soffer, *Acta Phys. Polon.* **B29**, 1303 (1998).

[59] P. Taxil and J. M. Virey, *Phys. Rev.* **D 55**, 4480 (1997); *Phys. Lett.* **B522**, 89 (2001).

[60] P. Taxil, J. M. Virey, *Phys. Lett.* **B364** (1995) 181; *Phys. Rev.* **D55** (1997) 4480.

[61] P. Taxil, J. M. Virey, *Phys. Lett.* **B383** (1996) 355; *Phys. Lett.* **B441** (1998) 376.

[62] P. Taxil, E. Tugcu, J. M. Virey, *Eur. Phys. J.* **C24** (2002) 149.

[63] C. Bourelly, et al., *Phys. Rep.* **177** (1989) 319; P. Taxil, *Polarized Collider Workshop, AIP Conf. Proc.* **223**, ed. J. Collins, S. F. Heppelmann, R. W. Robinett, p. 169 (1991); M. J. Tannenbaum, *Polarized Collider Workshop, AIP Conf. Proc.* **223**, ed. J. Collins, S. F. Heppelmann, R. W. Robinett, p. 201 (1991).

[64] B. Abott, et al. (DØ Collaboration), *Phys. Rev. Lett.* **82** (1999) 2457.

[65] J. D. Lykken, *Snowmass 1996*,ed. D. G. Cassel, L. Trindle Gennari, R. H. Siemann, p. 891; J. L. lopez, D. V. Nanopoulos, *Phys. Rev.* **D55** (1997) 397; K. S. Babu, C. Kolda, J. March-Russell, *Phys. Rev.* **D54** (1996) 4635; A. E. Fraggi, M. Masip, *Phys. Lett.* **B388** (1996) 524.

[66] K. Agashe, M. Graesser, I. Hinchliffe, M. Suzuki, *Phys. Lett.* **B385** (1996) 218; H. Georgi, S. L. Glashow, *Phys. Lett.* **B387** (1996) 341.

[67] M. Cvetič, et al., *Phys. Rev.* **D56** (1997) 2861.

[68] E. Courant, *Proc. of the RIKEN-BNL Research Center Workshop*, April 1998, BNL Report 65615, p. 275.

[69] T. Gehrmann, D. Maître, D. Wyler, *Nucl. Phys* **B703** (2004) 147.

[70] B. Abott, et al. (DØ Collaboration), *Phys. Rev. Lett.* **83** (1999) 4937; T. Affolder, et al. (CDF Collaboration), *Phys. Rev. Lett.* **88** (2002) 041801.

[71] P. Steinberg et al., "Expression of Interest for a Comprehensive New Detector at RHIC II", Presentation to the BNL PAC, BNL, September 8, 2004 (available at http://www.bnl.gov/HENP/docs/pac0904/bellwied_eoi_r1.pdf, unpublished).

[72] G. Bozzi, B. Fuks, M. Klasen, *Preprint LPSC 04-091*; *hep-ph/0411318*.

[73] C. Bourelly, J. Soffer, *Phys. Lett.* **B314** (1993) 132; *Nucl. Phys.* **B423** (1994) 329; P. Chiappetta, J. Soffer, *Phys. Lett.* **B152** (1985) 126.

[74] D. Boer, *Phys. Rev.* **D62** (2000) 094029.

[75] S. Kovalenko, I. Schmidt, J. Soffer, *Phys. Lett.* **B503** (2001) 313.

[76] G. L. Kane, G. A. Ladinsky, C.-P. Yuan, *Phys. Rev.* **D45** (1992) 124.

[77] A. Ogawa, V. L. Rykov, N. Saito, *Proc. of the 14th Int. Symp. on Spin Physics, AIP Conf. Proc* **570**, ed. T. Nakamura, p. 379 (2000); V. L. Rykov, *hep-ex/9908050*.

[78] R. Escribano, E. Masso, *Nucl. Phys.* **B429** (1994) 19.

[79] J. Soffer, *Nucl. Phys. (Proc. Suppl.)* **64** (1998) 143.

[80] T. Roser, W. Fischer, M. Bai, F. Pilat, “RHIC Collider Projections (FY2005-FY2008)”, http://www.rhichome.bnl.gov/RHIC/Runs/RhicProjections/pdf (Last update on 16 August 2004).

[81] J. Tojo et al., *Phys. Rev. Lett.* **89**, 052302 (2002).

[82] O. Jinnouchi et al., RHIC/CAD Acc. Phys. Note 171 (2004),

[83] T. Wise et al., and H. Okada et al., Spin2004 Proceedings, Trieste, Italy, to be published; and talks in http://www.ts.infn.it/events/SPIN2004/.

[84] N. Akchurin et al., *Phys. Rev.* **D48**, 3026 (1993).